JOC Article

A Combined Experimental and Theoretical Study of the Polar [3 + 2] Cycloaddition of Electrophilically Activated Carbonyl Ylides with Aldehydes and Imines

Ghenia Bentabed-Ababsa,[†,‡] Aicha Derdour,[‡] Thierry Roisnel,[§] Jose A. Sáez,[¶] Patricia Pérez,[⊥] Eduardo Chamorro,[⊥] Luis R. Domingo,*[,¶] and Florence Mongin*[,†]

Chimie et Photonique Moléculaires, UMR 6510 CNRS, Université de Rennes 1, Bâtiment 10A, Case 1003, Campus Scientifique de Beaulieu, 35042 Rennes, France, Laboratoire de Synthèse Organique Appliquée, Faculté des Sciences de l'Université, BP 1524 Es-Senia, Oran 31000, Algeria, Centre de Diffractométrie X, Sciences Chimiques de Rennes, UMR 6226 CNRS, Université de Rennes 1, Bâtiment 10B, Campus Scientifique de Beaulieu, F-35042 Rennes Cedex, France, Departamento de Química Orgánica, Universidad de Valencia, Dr. Moliner 50, 46100 Burjassot, Valencia, Spain, Facultad de Ecología y Recursos Naturales, Departamento de Ciencias Químicas, Laboratorio de Química Teórica, Universidad Andres Bello, Av. República 275, 8370146 Santiago, Chile

domingo@utopia.uv.es; florence.mongin@univ-rennes1.fr

Received December 11, 2008

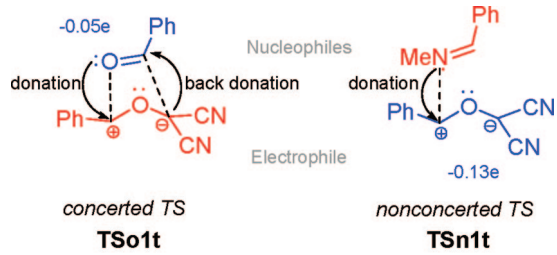

Reverse net CT at the reactions with aldehydes

Numerous 2,5-diaryl-1,3-dioxolane-4,4-dicarbonitriles and 2,4-diphenyl-1,3-oxazolidine-5,5-dicarbonitriles have been synthesized by [3 + 2] cycloaddition reactions between carbonyl ylides generated from epoxides and aldehydes or imines. In contrast to the use of aldehydes (3,4,5-trimethoxybenzaldehyde, piperonal, 1-naphthaldehyde, indole-3-carboxaldehyde, furan-2-carboxaldehyde, and thiophene-2-carboxaldehyde), the reactions performed with imines (*N*-(phenylmethylene)methanamine, *N*-(1,3-benzodioxol-5-ylmethylene)propylamine, *N*-(1,3-benzodioxol-5-ylmethylene)butylamine, and *N*-(1,3-benzodioxol-5-ylmethylene)benzylamine) proceed diastereoselectively. The effect of microwave irradiation on the outcome of the reaction was studied. The mechanism of these [3 + 2] cycloaddition reactions has been theoretically investigated using DFT methods. These cycloadditions, which have one-step mechanisms, consist of the nucleophilic attack of the aldehyde oxygen or imine nitrogen on the carbonyl ylide. For the reaction with aldehydes, a back-donation effect is responsible for the unexpected reverse charge transfer found at the transition structure. The analysis of the reactivity indexes indicates that the large electrophilic character of the carbonyl ylides induces them to act as strong electrophiles in these polar [3 + 2] cycloaddition reactions.

Introduction

Cycloaddition reactions are fundamental synthetic processes, with both synthetic and mechanistic interest in organic chemistry. Among them, 1,3-dipolar cycloadditions, the general concept of which was introduced by Huisgen and co-workers in the 1960s,[1] are versatile tools for building five-membered heterocycles.[2]

The 1,3-dioxolane[3] and oxazolidine[4] moieties represent important skeletons present in molecules endowed with biological activities. Derivatives can be synthesized by reaction of

* To whom correspondence should be addressed. Fax: +34 96 354 4328 (L.R.D.), +33 2 2323 6955.
† Chimie et Photonique Moléculaires, Université de Rennes 1.
‡ Faculté des Sciences de l'Université.
§ Centre de Diffractométrie X, Université de Rennes 1.
¶ Universidad de Valencia.
⊥ Universidad Andres Bello.

(1) Huisgen, R.; Grashey, R.; Sauer, J. In *The Chemistry of Alkenes*; Interscience: New York, 1964.

10.1021/jo8027104 CCC: $40.75
Published on Web 02/06/2009

SCHEME 1. Thermal Ring Opening of the Epoxide 1a and Cycloaddition Reaction between CYa and *N*-Methylisatin

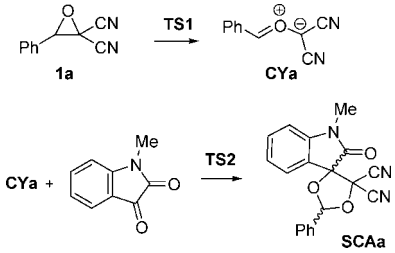

carbonyl ylides, generated by thermal electrocyclic ring opening of epoxides, with π-bonds of aldehydes[5] and imines.[6]

Current understanding of the underlying principles in reactions such as 1,3-dipolar cycloaddition has grown from a fruitful interplay between theory and experiment.[2] Through a recent study of the [3 + 2] cycloaddition reaction between carbonyl ylides and ketones in order to synthesize spirocyclic dioxolane indolinones,[7] we have embarked on theoretical calculations using DFT methods to depict the mechanism of these reactions using carbonyl ylides generated from epoxides. These reactions are domino processes that comprise two consecutive reactions (see Scheme 1).[7] The first one is the thermal ring opening of the epoxide **1a** to yield the carbonyl ylide intermediate **CYa**, whereas the second reaction is a concerted [3 + 2] cycloaddition of **CYa** with the ketone function of *N*-methylisatin to yield the final [3 + 2] spirocycloadducts **SCAa**. The activation energy associated with the thermal ring opening of the epoxide **1a**, 26.9 kcal/mol, proved to be slightly higher than that associated with the thermal opening of the cyclopropane ring on the 2,2-dimethoxy-3,3-dicyanospiro[cyclopropane-1,9′-[9*H*]fluorene recently reported by Warkentin, 24.4 kcal/mol.[8] However, the formation of the corresponding carbonyl ylide **CYa** was less endothermic, 11.7 kcal/mol, than the corresponding zwitterion intermediate, 22.8 kcal/mol. Interestingly, the zwitterion proposed by Warkentin was captured by benzaldehyde to yield a formally [3 + 2] cycloadduct, which showed the same regioselectivity as that found on the reaction of **CYa** with isatin.

Although the cycloaddition has a lower activation energy than that for the opening of the epoxide, the large endothermic character of the formation of the intermediate **CYa** together with the bimolecular nature of the cycloaddition makes this reaction the rate-limiting step of the overall domino process. The energetic results indicated that the [3 + 2] cycloaddition reaction presents a poor stereoselectivity and a large regio- and chemoselectivity, in agreement with the experimental results. The most favorable regioisomeric channels were associated with the nucleophilic attack of the isatin carbonyl oxygen atom to the phenyl-substituted carbon atom of the carbonyl ylide **CYa**. The larger electrophilicity of the carbonyl ylide **CYa**, $\omega = 4.29$ eV, with respect to *N*-methylisatin, $\omega = 2.66$ eV, allowed us to explain the nucleophilic attack of the carbonyl oxygen of the isatin to the phenyl-substituted carbon atom of **CYa**. However, a charge transfer (CT) analysis at the transition state structures (TSs) showed a slight net CT to the ketone framework.

If reactions between carbonyl ylides, generated by thermal electrocyclic ring opening of epoxides, with π-bonds of aldehydes[5a,b] and imines[6] have previously been described with similar regiospecificity and stereoselectivity, the identification of the *cis* and *trans* cycloadduct products has not been studied unequivocally. Here we describe similar syntheses[9] but most of all the structural analysis of the cycloadducts as well as their formation mechanism. The discrepancy between the electrophile/nucleophile interaction and the CT observed at the TSs of the cycloaddition of the carbonyl ylide **CYa** with *N*-methylisatin has encouraged us to perform subsequent studies on the mechanism of these [3 + 2] cycloaddition reactions.

Results and Discussion

Synthetic Aspects. Reactions were first carried out between 2,2-dicyano-3-(4-substituted)phenyloxiranes **1a**−**c**[10] and benzaldehydes **2** (1 molar equiv) in order to get 2,5-diphenyl-1,3-dioxolane-4,4-dicarbonitriles (Table 1). The conversion to the derivatives **3**−**5** using 3,4,5-trimethoxybenzaldehyde (**2a**) was monitored by NMR and showed that the reactions carried out in refluxing toluene were completed after 35−68 h, depending on the R^1 group on the epoxide **1**. The *cis* products **3a**−**5a** were isolated from the crude mixture by recrystallization from petrol/Et_2O in yields ranging from 40 to 52% and identified by NMR. NOESY, HMBC, and HMQC sequences were performed on $(CD_3)_2CO$ solutions which allowed for the assignments of the ^1H and ^{13}C NMR signals. The NOESY experiment showed the relationship between H2 (singlets at 6.59, 6.57, and 6.53 ppm for **3a**, **4a**, and **5a**, respectively) and H2′-H6′ (at 7.80, 7.74, and 7.68 ppm), and between H2 and H5 (singlets at 6.04, 6.00, and 5.99 ppm) (see Table 1, **a**). Compound *cis*-**5a** was then identified unequivocally by X-ray structure analysis. The *trans* compounds **3b**−**5b** were identified using ^1H NMR spectra of enriched fractions. The diastereoisomeric ratios were determined from ^1H NMR spectra of the crude mixtures. The *cis* products predominate over the *trans* with about 3/1 (**a/b**) ratios.

A rising number of articles have advocated the use of microwave technology in organic synthesis. Long reaction times

(2) (a) *1,3-Dipolar Cycloaddition Chemistry*; Padwa, A., Ed.; Wiley: New York, 1984; Vols. 1,2. (b) Gothelf, K. V.; Jorgenson, K. A. *Chem. Rev.* **1998**, *98*, 863–909. (c) Harwood, L. M.; Vickers, R. J. In *The Chemistry of Heterocyclic Compounds: Synthetic Applications of 1,3-Dipolar Cycloaddition Chemistry Toward Heterocycles and Natural Products*; Padwa, A.,Pearson, W. H., Eds.; Wiley and Sons: New York, 2002.

(3) See for example: (a) Bera, S.; Malik, L.; Bhat, B.; Caroll, S. S.; Hrin, R.; MacCoss, M.; McMasters, D. R.; Miller, M. D.; Moyer, G.; Olsen, D. B.; Schleif, W. A.; Tomassini, J. E.; Eldrup, A. B. *Bioorg. Med. Chem.* **2004**, *12*, 6237–6247. (b) Liang, Y.; Narayanasamy, J.; Schinazi, R. F.; Chu, C. K. *Bioorg. Med. Chem.* **2006**, *14*, 2178–2189. (c) Wender, P. A.; Verma, V. A. *Org. Lett.* **2006**, *8*, 1893–1896. (d) Schmidt, M.; Ungvári, J.; Glöde, J.; Dobner, B.; Langner, A. *Bioorg. Med. Chem.* **2007**, *15*, 2283–2297.

(4) See for example: (a) Tuchscherer, G.; Grell, D.; Tatsu, Y.; Durieux, P.; Fernandez-Carneado, J.; Hengst, B.; Kardinal, C.; Feller, S. *Angew. Chem., Int. Ed.* **2001**, *40*, 2844–2848. (b) Cheng, Q.; Kiyota, H.; Yamaguchi, M.; Horiguchi, T.; Oritani, T. *Bioorg. Med. Chem. Lett.* **2003**, *13*, 1075–1077. (c) Botta, M.; Armaroli, S.; Castagnolo, D.; Fontana, G.; Pera, P.; Bombardelli, E. *Bioorg. Med. Chem. Lett.* **2007**, *17*, 1579–1583. (d) Pasteris, R. J.; Hanagan, M. A.; Shapiro, R. PCT Int. Appl. WO 2008013622 A2 20080131, 2008.

(5) (a) Robert, A.; Pommeret, J. J.; Foucaud, A. *Tetrahedron Lett.* **1971**, *12*, 231–234. (b) Robert, A.; Pommeret, J. J.; Foucaud, A. *Tetrahedron* **1972**, *28*, 2085–2097. Concerning the $Rh_2(OAc)_4$-catalyzed synthesis of 2,5-diaryl-1,3-dioxolane, see for example: (c) Jiang, B.; Zhang, X.; Luo, Z. *Org. Lett.* **2002**, *4*, 2453–2455. (d) Russell, A. E.; Brekan, J.; Gronenberg, L.; Doyle, M. P. *J. Org. Chem.* **2004**, *69*, 5269–5274. (e) Lu, C.-D.; Chen, Z.-Y.; Liu, H.; Hu, W.-H.; Mi, A.-Q. *Org. Lett.* **2004**, *6*, 3071–3074.

(6) (a) Pommeret, J. J.; Robert, A. *C.R. Acad. Sci. Paris, Ser. C* **1971**, *272*, 333–336. (b) Robert, A.; Pommeret, J. J.; Marchand, E.; Foucaud, A. *Tetrahedron* **1973**, *29*, 463–468.

(7) Bentabed-Ababsa, G.; Derdour, A.; Roisnel, T.; Sáez, J. A.; Domingo, L. R.; Mongin, F. *Org. Biomol. Chem.* **2008**, *6*, 3144–3157.

(8) Sliwnska, A.; Czardybon, W.; Warkentin, J. *Org. Lett.* **2007**, *9*, 695–698.

(9) Preliminary studies have previously been reported: Bentabed, G.; Rahmouni, M.; Mongin, F.; Derdour, A.; Hamelin, J.; Bazureau, J. P. *Synth. Commun.* **2007**, *37*, 2935–2948.

(10) Baudy, M.; Robert, A.; Foucaud, A. *J. Org. Chem.* **1978**, *43*, 3732–3736.

TABLE 1. Reactions between Epoxides 1 and Benzaldehydes 2

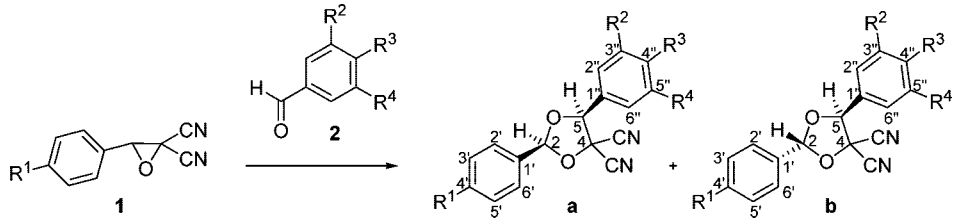

entry	R^1 (1)	aldehyde	a:b	conditions	a:b ratio[a]	isolated product, yield
1	H (**1a**)	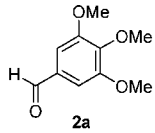 **2a**	**3a**:**3b**	toluene, reflux, 35 h	77/23	**3a**, 40%
				MW,[b] 60 W, 120°C, 45 min	68/32	**3a**, 49%
2	Cl (**1b**)		**4a**:**4b**	toluene, reflux, 68 h	72/28	**4a**, 42%
				MW,[b] 60 W, 120°C, 40 min	71/29	**4a**, 45%
3	OMe (**1c**)		**5a**:**5b**	toluene, reflux, 45 h	68/32	**5a**, 52%
				MW,[b] 60 W, 80°C, 35 min	70/30	**5a**, 55%
4	H (**1a**)	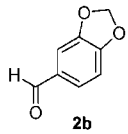 **2b**	**6a**:**6b**	toluene, reflux, 45 h	58/42	**6a**, 31%
				MW,[b] 60 W, 120°C, 40 min	66/34	**6a**, 25%
5	Cl (**1b**)		**7a**:**7b**	toluene, reflux, 72 h	60/40	**7a**, 28%
				MW,[b] 60 W, 120°C, 40 min	60/40	**7a**, 39%
6	OMe (**1c**)		**8a**:**8b**	toluene, reflux, 48 h	71/29	**8a**, 54%
				MW,[b] 60 W, 80°C, 30 min	67/33	**8a**, 40%

[a] Determined from the ^{1}H NMR spectra of the crude mixture. [b] Reactions performed without solvent.

often required for cycloaddition reactions could generally be reduced using this technique.[11] Thus, several experiments were performed using microwave irradiation at various powers and irradiation times.[12] The best conditions were obtained without solvent (power = 60 W), with significant reduction of reaction times (45 min instead of 35 h for **3** (R^1 = H), 40 min instead of 68 h for **4** (R^1 = Cl), and 35 min instead of 45 h for **5** (R^1 = OMe)) and similar **a/b** ratios (68/32 instead of 77/23 for **3** (R^1 = H), 71/29 instead of 72/28 for **4** (R^1 = Cl), and 70/30 instead of 68/32 for **5** (R^1 = OMe)) in comparison to reaction in toluene at reflux[13] (Table 1, entries 1−3).

Replacing 3,4,5-trimethoxybenzaldehyde (**2a**) with piperonal (**2b**) slightly disfavored the formation of the *cis* compounds **6a** and **7a** over the *trans* **6b** and **7b** (average **a/b** ratios of 62/38 for **6** against 72/28 for **3** (R^1 = H), and 60/40 for **7** against 71/29 for **4** (R^1 = Cl)), whereas the same ratio (69/31) was obtained for **8** and **5** (R^1 = OMe; entries 4−6). The *trans* **7b** and **8b** could only be identified using ^{1}H NMR spectra of enriched fractions, but crystals of **6b** suitable for X-ray structure analysis were obtained.

The *cis* products **6a**−**8a** were isolated from the crude mixture by recrystallization from petrol/Et_2O in moderate to medium yields. Their structures were elucidated as for compounds **3a**−**5a** using NMR experiments and confirmed by X-ray analysis.

In order to reach differently 5-substituted 2-(4-substituted phenyl)-1,3-dioxolane-4,4-dicarbonitriles, reactions were performed with 1-naphthaldehyde (**9**), indole-3-carboxaldehyde (**10**), furan-2-carboxaldehyde (**11**), and thiophene-2-carboxaldehyde (**12**) (1 molar equiv) (Table 2). The reactions were completed in refluxing toluene after reaction times of 35−84 h, depending on both the R group on the epoxide **1** and the nature of the aldehyde. The reactions were also carried out under microwave irradiation, allowing reaction times to be reduced from 54−84 h to 30−45 min.

The *cis* products **13a**−**15a** proved to be favored over the *trans* for the reactions carried out between 2,2-dicyano-3-(4-substituted)phenyloxiranes **1a**−**c**[10] and 1-naphthaldehyde (**9**). They were isolated from the crude mixtures by column chromatography over silica gel in yields ranging from 27 to 55% and identified by NMR. NOESY, HMBC, and HMQC sequences performed on the racemic **14a** allowed the assignments of the main ^{1}H and ^{13}C signals. The proximity between H2 and H5, in accordance with a *cis* stereochemistry, was shown by conducting the NOESY experiment in $CDCl_3$, after assignment of the singlets at 6.38 and 6.48 ppm[14] to H2 (correlation between H2 and H2′-H6′) and H5 (correlation between H5 and H2”), respectively (see Table 2, **a**). After identification of the *trans* compounds **13b**−**15b** from ^{1}H NMR spectra of the crude mixtures, the diastereoisomeric ratios were calculated using the integration. The **a/b** ratio is about 63/37 when R = H, against 71/29 when R = Cl and OMe, and is slightly favored using classical heating conditions (entries 1−3).

The reactions carried out under classical heating conditions between 2,2-dicyano-3-(4-substituted)phenyloxiranes **1a**−**c**[10] and indole-3-carboxaldehyde (**10**) resulted in different diastereoisomeric ratios than using 1-naphthaldehyde (**9**). Indeed, 50/50 (**16**, R = H), 43/57 (**17**, R = Cl), and 84/16 (**18**, R = OMe) were obtained as *cis*/*trans* ratios using the heterocyclic aldehyde against 65/35 (**13**, R = H), 75/25 (**14**, R = Cl), and 76/24 (**15**, R = OMe) for the nonheterocyclic one. Recourse to microwave irradiation favors the formation of **16a**−**17a** over **16b**−**17b** but

(11) (a) de la Hoz, A.; Díaz-Ortiz, A.; Langa, F. In *Microwave in Organic Synthesis*, 1st ed.; Loupy, A., Ed.; Wiley-VCH: Weinheim, Germany, 2002; Chapter 9. (b) Bougrin, K.; Soufiaoui, M.; Bashiardes, G. In *Microwave in Organic Synthesis*, 2nd ed.; Loupy, A., Ed.;Wiley-VCH: Weinheim, Germany, 2006; Vol. 1, Chapter 11.

(12) Using a monomode reactor (Prolabo Synthewave 402) with accurate control of power and temperature (infrared detection).

(13) Note that the reactions did not proceed cleanly when the reactants were heated without solvent in an oil bath.

(14) Note that H5 is shifted towards high fields when a 1-naphthyl group is present at the 5 position of the dioxolane ring.

TABLE 2. Reactions between Epoxides 1 and Aldehydes 9−12

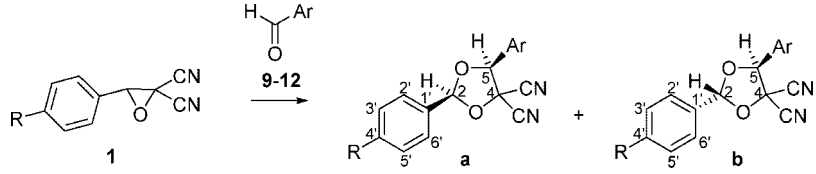

entry	R (**1**)	aldehyde	**a**:**b**	conditions	**a**:**b** ratio[a]	isolated product(s), yield(s)
1	H (**1a**)	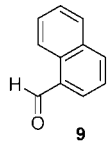 **9**	**13a**:**13b**	toluene, reflux, 80 h	65/35	**13a**, 27%
				MW,[b] 90 W, 120°C, 40 min	62/38	**13a**, 35%
2	Cl (**1b**)		**14a**:**14b**	toluene, reflux, 72 h	75/25	**14a**, 32%
				MW,[b] 90 W, 120°C, 40 min	63/37	**14a**, 42%
3	OMe (**1c**)		**15a**:**15b**	toluene, reflux, 57 h	76/24	**15a**, 48%
				MW,[b] 90 W, 80°C, 30 min	71/29	**15a**, 55%
4	H (**1a**)	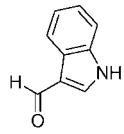 **10**	**16a**:**16b**	toluene, reflux, 84 h	50/50	**16a**, 40%
				MW,[b] 90 W, 120°C, 45 min	60/40	**16a**, 42%
5	Cl (**1b**)		**17a**:**17b**	toluene, reflux, 80 h	43/57	**17a**, 37%
				MW,[b] 90 W, 120°C, 45 min	76/24	**17a**, 39%
6	OMe (**1c**)		**18a**:**18b**	toluene, reflux, 54 h	84/16	**18a**, 46%
				MW,[b] 120 W, 80°C, 40 min	66/34	**18a**, 30%
7	H (**1a**)	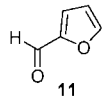 **11**	**19a**:**19b**	toluene, reflux, 50 h	66/34	**19a**, 36%
8	Cl (**1b**)		**20a**:**20b**	toluene, reflux, 40 h	67/33	**20b**, 21%
9	OMe (**1c**)		**21a**:**21b**	toluene, reflux, 35 h	65/35	**21b**, 15%
10	H (**1a**)	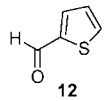 **12**	**22a**:**22b**	toluene, reflux, 48 h	73/27	**22a**, 40%; **22b**, 20%
11	Cl (**1b**)		**23a**:**23b**	toluene, reflux, 41 h	74/26	**23a**, 45%; **23b**, 25%
12	OMe (**1c**)		**24a**:**24b**	toluene, reflux, 36 h	62/38	**24a**, 50%; **24b**, 20%

[a] Determined from the ^{1}H NMR spectra of the crude mixture. [b] Reactions performed without solvent.

disfavors the formation of **18a** over **18b** (entries 4−6). The *cis* products were isolated from the crude mixture by column chromatography over silica gel in 30−46% yields and were identified by NMR as before, by identifying a correlation relation between H2 and H5 (see Table 2, **a**). The structure of **17a** was confirmed by X-ray analysis of crystals obtained by slowly evaporating an acetone solution. Products **16b**−**17b** were identified using ^{1}H and ^{13}C NMR spectra of enriched fractions, and **18b** was identified from the ^{1}H NMR spectra of the crude mixture.

When furan-2-carboxaldehyde (**11**) (entries 7−9) and thiophene-2-carboxaldehyde (**12**) (entries 10−12) were similarly involved in the reactions with 2,2-dicyano-3-(4-substituted)phenyloxiranes **1a**−**c**,[10] rather similar **a**/**b** ratios were obtained, that is to say 66/34 (**19**, R = H), 67/33 (**20**, R = Cl), and 65/35 (**21**, R = OMe) using furan **11**, and 73/27 (**22**, R = H), 74/26 (**23**, R = Cl), and 62/38 (**24**, R = OMe) using thiophene-2-carboxaldehyde (**12**). The products **19a**, **20b**, **21b**, **22a**,**b**, **23a**,**b**, and **24a**,**b** were isolated from the crude mixtures by column chromatography over silica gel and/or recrystallization from petrol/Et_2O, and all the structures were first determined on the basis of ^{1}H and ^{13}C NMR chemical shifts. This was consistent with a complete NMR study including HMBC, HMQC, and NOESY experiments performed on **19a**. In addition, attempts to get crystals suitable for X-ray analysis from an acetone solution were successful for *trans*-**20b** and *cis*-**24a**.

Reactions were finally carried out between 2,2-dicyano-3-(4-substituted)phenyloxiranes **1a**−**d**[10] and imines **25**[15] (1 molar equiv) in order to get substituted 2,4-diphenyloxazolidine-5,5-dicarbonitriles (Table 3). The conversion to the derivatives **26**−**28** using *N*-(phenylmethylene)methanamine (**25a**), **30**−**32** using *N*-(1,3-benzodioxol-5-ylmethylene)propylamine (**25b**), **34**−**36** using *N*-(1,3-benzodioxol-5-ylmethylene)butylamine (**25c**), and **38**−**40** using *N*-(1,3-benzodioxol-5-ylmethylene)benzylamine (**25d**) were monitored by NMR and showed that the reactions carried out in refluxing toluene were finished in 5−40 h with imines **25**, against 35−72 h with benzaldehydes **2**. The conversion to derivatives **29**, **33**, **37**, and **41** proved possible by reaction of imines **25** with 2,2-dicyano-3-(4-nitro)phenyloxirane (**1d**), an epoxide unable to react with benzaldehydes **2**. Also in contrast to what has been observed using aldehydes, the ^{1}H NMR spectra of the crude mixtures showed that *cis* diastereoisomers were always mainly formed with ratios >90/10. The main compounds **26a**−**41a** were isolated from the crude reaction mixtures by chromatography over silica gel and/or recrystallization from Et_2O. Yields were satisfactory for R^1 = H, Cl, OMe (48−80%), and lower for R^1 = NO_2 (18−40%). Even if reaction times were shorter using imines, the reactions were carried out under microwave irradiation without significant changes (32−85% for R^1 = H, Cl, OMe, and 18−33% for R^1 = NO_2). As before, recourse to NMR HMBC, HMQC, and

(15) Chérouvrier, J.-R.; Carreaux, F.; Bazureau, J. P. *Tetrahedron Lett.* **2002**, *43*, 3581–3584.

TABLE 3. Reactions between Epoxides 1 and Imines 25

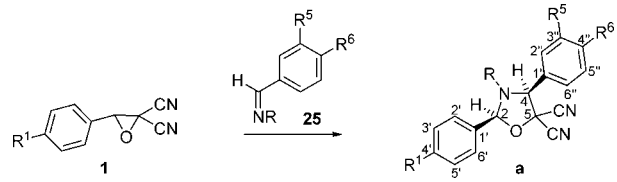

entry	R^1 (**1**)	imine	conditions	isolated product, yield
1	H (**1a**)	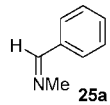 **25a**	toluene, reflux, 24 h	**26a**, 52%
			MW,[b] 120 W, 125°C, 55 min	**26a**, 35%
2	Cl (**1b**)		toluene, reflux, 20 h	**27a**, 60%
			MW,[b] 120 W, 125°C, 50 min	**27a**, 48%
3	OMe (**1c**)		toluene, reflux, 5 h	**28a**, 78%
			MW,[b] 60 W, 80°C, 25 min	**28a**, 85%
4	NO_2 (**1d**)		toluene, reflux, 35 h	**29a**, 40%
			MW,[b] 150 W, 125°C, 60 min	**29a**, 33%
5	H (**1a**)	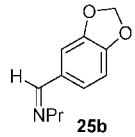 **25b**	toluene, reflux, 27 h	**30a**, 48%
			MW,[b] 120 W, 125°C, 55 min	**30a**, 32%
6	Cl (**1b**)		toluene, reflux, 25 h	**31a**, 59%
			MW,[b] 120 W, 125°C, 45 min	**31a**, 40%
7	OMe (**1c**)		toluene, reflux, 9 h	**32a**, 60%
			MW,[b] 60 W, 80°C, 30 min	**32a**, 80%
8	NO_2 (**1d**)		toluene, reflux, 45 h	**33a**, 35%
			MW,[b] 150 W, 125°C, 65 min	**33a**, 30%
9	H (**1a**)	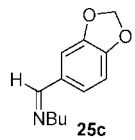 **25c**	toluene, reflux, 32 h	**34a**, 56%
			MW,[b] 120 W, 125°C, 60 min	**34a**, 40%
10	Cl (**1b**)		toluene, reflux, 32 h	**35a**, 59%
			MW,[b] 120 W, 125°C, 60 min	**35a**, 49%
11	OMe (**1c**)		toluene, reflux, 9 h	**36a**, 60%
			MW,[b] 60 W, 80°C, 30 min	**36a**, 75%
12	NO_2 (**1d**)		toluene, reflux, 65 h	**37a**, 18%
			MW,[b] 150 W, 125°C, 75 min	**37a**, 22%
13	H (**1a**)	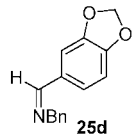 **25d**	toluene, reflux, 40 h	**38a**, 60%
			MW,[b] 120 W, 125°C, 70 min	**38a**, 42%
14	Cl (**1b**)		toluene, reflux, 37 h	**39a**, 50%
			MW,[b] 120 W, 125°C, 60 min	**39a**, 37%
15	OMe (**1c**)		toluene, reflux, 18 h	**40a**, 80%
			MW,[b] 60 W, 80°C, 35 min	**40a**, 70%
16	NO_2 (**1d**)		toluene, reflux, 72 h	**41a**, 27%
			MW,[b] 150 W, 125°C, 90 min	**41a**, 18%

[a] Determined from the ^{1}H NMR spectra of the crude mixture. [b] Reactions performed without solvent.

NOESY sequences allowed the assignments of ^{1}H and ^{13}C signals, as well as the detection of a correlation between H2 and H4 (see Table 3, **a**), in accordance with a *cis* stereochemistry. Compounds *cis*-**29a**, *cis*-**31a**−**33a**, and *cis*-**39a** were then identified unequivocally by X-ray structure analysis.

Theoretical Study of the [3 + 2] Cycloaddition Reactions of the Carbonyl Ylide CYa with Aldehydes and Imines. (A) Analysis Based on the Global and Local Reactivity Indexes at the Ground State of the Reagents. Recent studies devoted to Diels−Alder[16] and [3 + 2] cycloaddition[17] reactions have shown that the analysis of the global indexes defined within the context of conceptual DFT[18] is a powerful tool to understand the behavior of polar cycloadditions. In Table 4, we report the static global properties, namely, electronic chemical potential μ, chemical hardness η, global electrophilicity ω, and nucleophilicity N, of the carbonyl ylides **CYa**−**c**, the aromatic aldehydes **2a**−**c**, and the imines **25a** and **25e**.

The electronic chemical potentials, μ, of the carbonyl and imine derivatives, which range from −0.1434 to −0.1199 au, are higher than those for the carbonyl ylides, where μ values range from −0.1576 to −0.1746 au, indicating that along these [3 + 2] cycloadditions the net CT will take place from the carbonyl and imine derivatives to the carbonyl ylides.

The carbonyl ylide **CYa** has a high electrophilicity value,[19] ω = 4.29 eV. Electron-releasing (ER) substitution by a −OMe group decreases the electrophilicity of **CYc**, ω = 3.80 eV, while electron-withdrawing (EW) substitution by a Cl atom increases the electrophilicity of **CYb**, ω = 4.67 eV. Note that these carbonyl ylides present the larger electrophilicity of this series, indicating that along these [3 + 2] cycloaddition reactions they will act as strong electrophiles. Unsubstituted benzaldehyde (**2c**) and the corresponding methyl imine **25a** also have large

(16) (a) Domingo, L. R.; Aurell, M. J.; Perez, P.; Contreras, R. *Tetrahedron* **2002**, *58*, 4417–4423. (b) Pérez, P.; Domingo, L. R.; Aizman, A.; Contreras, R. In *Theoretical Aspects of Chemical Reactivity*; Toro-Labbé, A., Ed.; Elsevier Science: New York, 2007; Vol. 19, pp 139−201.

(17) Pérez, P.; Domingo, L. R.; Aurell, M. J.; Contreras, R. *Tetrahedron* **2003**, *59*, 3117–3125.

(18) (a) Geerlings, P.; De Proft, F.; Langenaeker, W. *Chem. Rev.* **2003**, *103*, 1793–1873. (b) Ess, D. H.; Jones, G. O.; Houk, K. N. *Adv. Synth. Catal.* **2006**, *348*, 2337–2361.

(19) Parr, R. G.; von Szentpaly, L.; Liu, S. *J. Am. Chem. Soc.* **1999**, *121*, 1922–1924.

TABLE 4. Electronic Chemical Potential (μ, in au), Chemical Hardness (η, in au), Global Electrophilicity (ω, in eV), and Global Nucleophilicity (N, in eV) Values of the Carbonyl Ylides CYa−c and the Aromatic Aldehydes 2a−c and Imines 25a and 25e (by decreasing values of ω)

entry	**compound** (R)		μ	η	ω	N
1	**CYb** (R^1 = Cl)	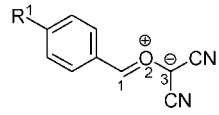	−0.1746	0.0889	4.67	3.16
2	**CYa** (R^1 = H)		−0.1693	0.0908	4.29	3.28
3	**CYc** (R^1 = OMe)		−0.1576	0.0890	3.80	3.62
4	**2c** (R^2 = R^3 = R^4 = H)	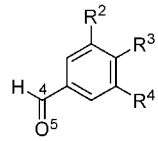	−0.1590	0.1923	1.79	2.18
5	**2a** (R^2 = R^3 = R^4 = OMe)		−0.1434	0.1719	1.63	2.88
6	**2b** (R^2R^3 = OCH_2O, R^4 = H)		−0.1392	0.1656	1.59	3.08
7	**25a** (R^5 = R^6 = H)	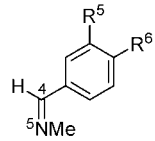	−0.1379	0.1964	1.32	2.70
8	**25e** (R^5R^6 = OCH_2O)		−0.1199	0.1705	1.15	3.54

electrophilicity values, ω = 1.79 and 1.32 eV, respectively, being classified as strong electrophiles within the electrophilicity scale.[16,17] Substitution on the aromatic ring by ER −OR groups decreases the electrophilicity of the carbonyl and imine derivatives.

The carbonyl ylides have very large nucleophilicity values,[20] N between 3.16 and 3.62 eV, respectively, and are also classified as strong nucleophiles. Note that the nucleophilicity is also sensitive to the substitution on the aromatic ring, the methoxy derivative **CYa** being the most nucleophilic species of the series given in Table 4. Interestingly, as can be concluded of the ω and N values, these carbonyl ylides could act as strong electrophiles and nucleophiles in polar cycloaddition reactions. Benzaldehyde (**2c**) and the imine **25a** have also a large nucleophilicity, which increases with the ER substitution on the phenyl ring. Thus, the imine **25e** is the best nucleophile of the PhCH=X(R) reagent subseries.

An analysis of the global indexes indicates that both reagents involved in these [4 + 3] cycloadditions can act as good electrophiles and nucleophiles in polar cycloadditions. It is expected that the more favorable polar interaction will take place between the strongest electrophilic reagent and the strongest nucleophilic one. Previously, we have proposed that the better interaction will take place between the pairs of reagents presenting the largest $\Delta\omega$,[16] that is, between reagents located at the opposite sides of the electrophilicity scale. In Diels−Alder reactions, we have shown that a reagent located above another reagent in the electrophilicity scale forces the last to behave as a nucleophile.[21] Therefore, it is expected that, in both reactions, **CYa** will act as the electrophile whereas **2c** and **25a** will act as nucleophiles.

Recent studies devoted to cycloaddition reactions with a polar character have shown that the analysis of the local electrophilicity index,[22] ω_k, at the electrophilic reagent and the nucleophilic Fukui function,[23] f_k^-, at the nucleophilic one allows one to explain the observed regioselectivity. Very recently, we have proposed the local nucleophilicity index, N_k,[24] which is able to measure the local nucleophilic activation between molecules. In this way, the ω_k and N_k at the carbonyl ylide **CYa**, at the aldehyde **2c**, and at the imine **25a** will be used to predict the best electrophile/nucleophile interaction in these polar cycloadditions and, therefore, to explain the regioselectivity experimentally observed.

TABLE 5. Local Electrophilicity, ω_k, and Nucleophilicity, N_k, Values (in eV) of the Carbonyl Ylide CYa, Benzaldehyde (2c), and the Imine 25a

	ω_k		N_k	
CYa	C1	C3	C1	C3
	1.30	0.45	0.46	1.13
2c	C4	O5	C4	O5
	0.47	0.35	0.10	1.52
25a	C4	N5	C4	N5
	0.25	0.30	0.11	0.50

The carbonyl ylide **CYa** has the largest electrophilic activation at the phenyl-substituted C1 carbon atom, ω_k = 1.30 eV, and the largest nucleophilic activation at the dicyano-substituted C3 carbon atom, N_k = 1.13 eV (see Table 5). Therefore, C1 and C3 will be the most electrophilic and nucleophilic centers, respectively, of these carbonyl ylides. This picture is in agreement with a heterolytic C1−C3 bond breaking of the epoxide **1a**, in which the phenyl-substituted C1 position becomes the carbocationic center while the dicyano-substituted C3 position turns into the carbanionic center.

The aldehyde **2c** has the largest electrophilic activation at the carbonyl C4 carbon atom, ω_k = 0.47 eV, and the largest nucleophilic activation at the carbonyl O5 oxygen atom, N_k = 1.52 eV, whereas the imine **25a** has both the largest electrophilic and nucleophilic activation sites at the imine N5 nitrogen atom, ω_k = 0.30 eV and N_k = 0.50 eV (see Table 5). Then, while the carbonyl C4 carbon is the most electrophilic center of **2c**, the N5 nitrogen is the most electrophilic center of the imine **25a**. In addition, the nucleophilic activation of the carbonyl O5 oxygen of **2c** is three times higher than that at the imine N5 nitrogen of **25a**. The results obtained for the imine **25a**, which locate the most nucleophilic and electrophilic centers over the

(20) Domingo, L. R.; Chamorro, E.; Perez, P. *J. Org. Chem.* **2008**, *73*, 4615–4624.
(21) (a) Domingo, L. R. *Eur. J. Org. Chem.* **2004**, 4788–4793. (b) Domingo, L. R.; Chamorro, E.; Perez, P. *J. Phys. Chem. A* **2008**, *112*, 4046–4053.
(22) Domingo, L. R.; Aurell, M. J.; Perez, P.; Contreras, R. *J. Phys. Chem. A* **2002**, *106*, 6871–6875.
(23) Parr, R. G.; Yang, W. *J. Am. Chem. Soc.* **1984**, *106*, 4049–4050.
(24) Pérez, P.; Domingo, L. R.; Duque, M.; Chamorro, E. *J. Mol. Struct. (THEOCHEM)* **2009**, *895*, 86−91.

same atom, are a consequence of the presence of the conjugated aromatic ring at the carbon atom, which modifies the electrophilic/nucleophilic behavior of the N5═C4 double bond.

For the [3 + 2] cycloaddition reaction between **CYa** and the aldehyde **2c**, the regioisomeric channels associated with the formation of the C1−O5 and C3−C4 bonds correspond to the approach that makes possible the interaction between the most electrophilic(A)/nucleophilic(B) centers of these reagents, respectively. If we consider the sum of the $\omega_k + N_k$ values at the two feasible interactions that take place along the **CYa** + **2c** reaction, 2.82 eV along the C1/O5 two-center interaction ($\omega_{kC1} + N_{kO5}$) and 1.60 eV ($N_{kC3} + \omega_{kC4}$) along the C3/C4 two-center interaction, we can see that the former is clearly favored. This analysis allows one to explain the fact that, at the more favorable regioisomeric **TSo1c** and **TSo1t**, the C1−O5 bond formation is more advanced than the C3−C4 one (see later).

(B) Mechanistic Study of the [3 + 2] Cycloaddition Reactions of the Carbonyl Ylide CYa with Benzaldehyde (2c) and the Imine 25a. For each one of these [3 + 2] cycloaddition reactions, four reactive channels have been studied. They are related to the two regioisomeric approaching modes of **CYa** to the aldehyde, **x** = **o**, or to the imine, **x** = **n**, named as **1** and **2**, and the two stereoisomeric approaching modes related to the *cis* or *trans* rearrangement of the two phenyl substituents on the final [3 + 2] cycloadducts, named as **c** and **t**. Note that the carbonyl ylide **CYa** can adopt the *E* or *Z* configuration by the restricted rotation of the C1−O2 bond. While (*E*)-**CYa** adopts a planar rearrangement,[7] (*Z*)-**CYa** is twisted as a consequence of the hindrance between the phenyl and one cyano group. This hindrance makes (*Z*)-**CYa** 8.6 kcal/mol higher in energy than (*E*)-**CYa**. In addition, the barrier height associated with the C1−O2 bond rotation is very large, 27.1 kcal/mol. Consequently, only the *E* configuration of the carbonyl ylide **CYa** was considered in the present study. An analysis of the stationary points associated with the reaction channels of these cycloadditions indicates that they have a one-step mechanism. Therefore, eight TSs and eight cycloadducts were located and characterized (see Scheme 2).

The activation energies of the most favorable reaction channels of these cycloadditions have very low values; 2.6 kcal/mol for **TSo1c** and 2.8 kcal/mol for **TSn1t** (see Table 6). The cycloadditions present a very low stereoselectivity in the case of aldehydes. For the reaction of **CYa** with the imine **25a**, the computed *trans* stereoselectivity is opposite to that found experimentally. Further single-point calculations at the MP3/6-31G*//B3LYP/6-31G* yielded a *trans* stereoselectivity similar to that obtained at the DFT level. All these [3 + 2] cycloaddition reactions present a total regioselectivity, being the more unfavorable regioisomeric TSs between 10 and 12 kcal/mol higher in energy. In addition, all cycloadditions are strongly exothermic: between −30.0 and −36.0 kcal/mol. These energy results are similar to those recently obtained for the [3 + 2] cycloaddition reaction of the carbonyl ylide **CYa** with *N*-methylisatin (see Scheme 1).[7]

As all these [3 + 2] cycloaddition reactions have a polar character and solvent can stabilize some species, solvent effects of toluene were considered through single-point energy calculations over the gas-phase-optimized geometries using the PCM method. Solvent effects stabilize all species between 2 and 7 kcal/mol (see Table 6), with the reagents being more stabilized than the TSs. As a consequence, the activation barrier for the cycloadditions increases by 2.0 and 1.0 kcal/mol. In addition, solvent effects do not change the gas phase low stereo- and the large regioselectivity found. Therefore, solvent effects appear to have little influence over the [3 + 2] cycloaddition reactions, remaining the *trans* selectivity for the reaction with the imine **25a**. Further thermodynamic calculations in toluene showed that **TSn1t** remains 2.6 kcal/mol in free energy below **TSn1c** (see Table 7).

One of the reviewers proposed that *under the rather severe reaction conditions the imine E/Z interconversion should take place populating the less stable (Z) imine stereoisomer that is presumably a more reactive dipolarophile*. In order to probe this suggestion, the TSs associated with the *cis* and *trans* approach modes of the imine **25a** in the *Z* configuration to the carbonyl ylide **CYa**, **TSn1c-Z** and **TSn1t-Z** were optimized.

SCHEME 2. Reaction Channels Studied for the Cycloaddition Reaction between CYa and 2c or 25a

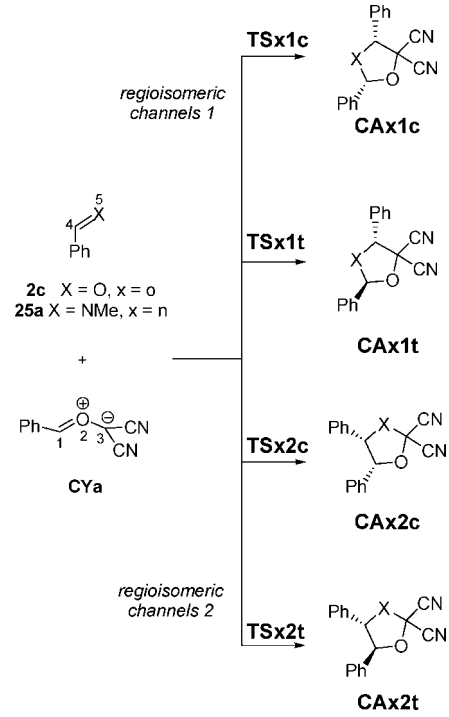

TABLE 6. Total (*E*, in au) and Relative (Δ*E*, in kcal/mol) Energies, in Gas Phase and in Toluene, of the Stationary Points Involved in the [3 + 2] Cycloaddition Reactions of the Carbonyl Ylide CYa with Benzaldehyde (2c) and the Imine 25a

	E	Δ*E*	$E_{toluene}$	$\Delta E_{toluene}$
CYa	−569.289033		−569.298872	
2c	−345.573442		−345.577940	
TSo1c	−914.858355	2.6	−914.869424	4.6
TSo1t	−914.858333	2.6	−914.869037	4.9
TSo2c	−914.841138	13.4	−914.850215	16.7
TSo2t	−914.841635	13.1	−914.850095	16.8
CAo1c	−914.913839	−32.2	−914.922338	−28.6
CAo1t	−914.910561	−30.2	−914.918724	−26.3
CAo2c	−914.904879	−26.6	−914.912830	−22.6
CAo2t	−914.909770	−29.7	−914.917550	−25.6
25a	−365.008701		−365.011670	
TSn1c	−934.290181	4.7	−934.300925	6.0
TSn1t	−934.293307	2.8	−934.304485	3.8
TSn2c	−934.274360	14.7	−934.282835	17.4
TSn2t	−934.274440	14.6	−934.282450	17.6
CAn1c	−934.355789	−36.4	−934.363842	−33.5
CAn1t	−934.348124	−31.6	−934.356115	−28.6
CAn2c	−934.350452	−33.1	−934.358006	−29.8
CAn2t	−934.355171	−36.0	−934.362370	−32.5

TABLE 7. Total and Relative (Relative to TSo1t and TSn1t) Enthalpies (*H*, in au, and Δ*H*, in kcal/mol), Entropies (*S* and Δ*S*, in eu), and Free Energies (*G*, in au, and Δ*G*, in kcal/mol) at 110 °C in Toluene of the TSs Involved in the [3 + 2] Cycloaddition Reactions of the Carbonyl Ylide CYa with Benzaldehyde (2c) and the Imine 25a

	H	Δ*H*	*S*	Δ*S*	*G*	Δ*G*
TSo1c	−914.616511	−0.1	165.36	1.5	−914.717702	−0.7
TSo1t	−914.616273	0.0	163.83	0.0	−914.716527	0.0
TSn1c	−934.007402	2.3	180.64	−0.8	−934.117946	2.6
TSn1t	−934.011091	0.0	181.41	0.0	−934.122104	0.0
TSn1c-Z	−934.011051	0.0	185.50	4.1	−934.124567	−1.5
TSn1t-Z	−934.011018	0.0	176.33	−5.1	−934.118923	2.0

However, **TSn1c-Z** and **TSn1t-Z** were located on the potential energy surface 1.0 and 1.5 kcal/mol above **TSn1t** (the total energies and geometries of these TSs are given is Supporting Information). For the reaction of the carbonyl ylide **CYa** with isatin, we found that thermodynamic calculations at the reaction conditions do not modify the regio- and chemoselectivity of the reaction. In order to probe if these calculations have some incidence on the *cis*/*trans* stereochemistry of the reactions, the free energies of the TSs involved in these cycloadditions were calculated at 110 °C in toluene. The results are summarized in Table 7. A comparison of the free energies of the TSs involved in the cycloaddition of **CYa** with benzaldehyde (**2c**) and the imine **25a** with the *E* configuration indicates that the inclusion of the thermal corrections and entropy to the free energies does not modify the stereochemistry found with the gas-phase electronic energies. However, when the thermodynamic calculations were performed at the TSs of the imine **25a** with the *Z* configuration, an interesting result was found. Now, **TSn1c-Z** is located −1.5 kcal/mol below **TSn1t** in free energy, in agreement with the *trans* selectivity found experimentally. An analysis of the enthalpies and entropies of the TSs indicates that the large entropy associated with **TSn1c-Z** together with the high reaction temperature, 110 °C, is responsible for the *trans* selectivity.

The geometries of the TSs associated with the [3 + 2] cycloaddition reactions between **CYa** and benzaldehyde (**2c**) are given in Figure 1, while those associated with the reaction with the imine **25a** are given in Figure 2. At the most favorable regioisomeric TSs, the lengths of the C1−X5 (X = O or N) bonds are shorter than the C3−C4 ones, a similar result to that found for the reaction of **CYa** with *N*-methylisatin. The extent of the asynchronicity of the bond formation in a cycloaddition reaction can be measured through the difference between the lengths of the two σ bonds that are being formed in the reaction (*i.e.*, Δ*r* = dist1 − dist2). The asynchronicity at the TSs is 0.52 at **TSo1c**, 0.38 at **TSo1t**, 0.01 at **TSo2c**, 0.01 at **TSo2t**, 0.66 at **TSn1c**, 0.82 at **TSn1t**, 0.13 **TSn2c**, and 0.11 at **TSn2t**. Two conclusions can be drawn from these values: (i) the TSs associated with the more favorable regioisomeric channels **1** are far more asynchronous than those associated with the channels **2**; and (ii) the TSs associated with the cycloadditions involving the imine **25a** are more asynchronous than those involving the aldehyde **2c**.

The electronic structure of the TSs involved in the more favorable regioisomeric channels of these [3 + 2] cycloaddition reactions was analyzed using the Wiberg bond order[25] (BO), the natural charges obtained by a NBO (natural bond order) analysis, and the topological analysis of the electron localization function (ELF). The C1−X5 (X = O or N) BO values at the TSs are 0.32 at **TSo1c**, 0.32 at **TSo1t**, 0.40 at **TSn1c**, and 0.34 at **TSn1t**, while the C3−C4 BO values are 0.20 at **TSo1c**, 0.24 at **TSo1t**, 0.14 at **TSn1c**, and 0.01 at **TSn1t**. At these TSs, the C1−X5 bond formation is more advanced than the C3−C4 one, in clear agreement with the analysis carried out with the local electrophilicity and nucleophilicity indexes. The [3 + 2] cycloaddition reactions involving the imine **25a** are more advanced and more asynchronous than those involving the aldehyde **2c**.

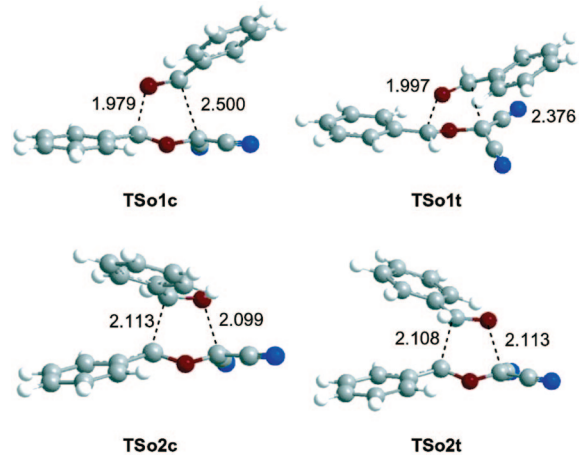

FIGURE 1. Transition structures involved in the reaction of the carbonyl ylide **CYa** with benzaldehyde (**2c**).

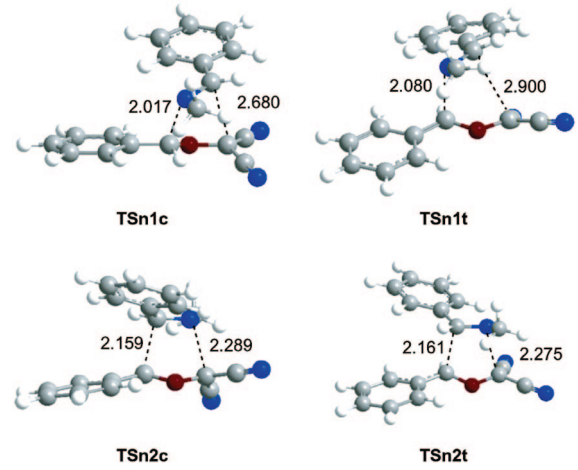

FIGURE 2. Transition structures involved in the reaction of the carbonyl ylide **CYa** with the imine **25a**.

An analysis of the atomic movement associated with the unique imaginary frequency of **TSn1t** indicated that it is mainly associated with the C1−N5 bond formation. The IRC from **TSn1t** to **CAn1t** indicates that this cycloaddition has a *two-stage* mechanism;[26] that is, while at the first stage of the reaction only the C1−N5 bond is being formed, the second stage is associated with the C3−C4 bond formation. We want to remark the **HPn1t** structure located at the half of IRC where the C1−N5 bond formation is very advanced, 1.697 Å, whereas the C3−C4 bond formation is very delayed, 2.778 Å. At **HPn1t**, the BO values of the C1−N5 and C3−C4 forming bonds are 0.74 and 0.22, respectively. On the other hand, the IRC from the

(25) Wiberg, K. B. *Tetrahedron* **1968**, *24*, 1083–1096.

(26) Domingo, L. R.; Saéz, J. A.; Zaragozá, R. J.; Arnó, M. *J. Org. Chem.* **2008**, *73*, 8791–8799.

asynchronous **TSo1t** to **CAo1t** shows the concerted nature of this cycloaddition. Along the reaction, the C1−O5 bond formation is slightly more advanced than the C3−C4 one.

The natural population analysis (NPA) allows the evaluation of the CT and its direction at these [3 + 2] cycloaddition reactions. The B3LYP/6-31G* natural atomic charges at the TSs associated with the most favorable regioselective channels were shared between the fragments of the carbonyl ylide **CYa** and the PhCH═X(R) derivatives **2c** and **25a**. The net charge at the carbonyl ylide fragment at these TSs is predicted to be +0.03e at **TSo1c**, +0.05e at **TSo1t**, and −0.13e at **TSn1c** and**TSn1t**. Along the IRC from **TSn1t** to **CAn1t**, the CT increases until it reaches −0.20e at **HPn1t**; after this point, the CT decreases due to a back-donation process from the carbonyl ylide to the imine. Some interesting conclusions can be obtained from these results: (i) First, these values indicate that there is a change in the direction of the flux of the net CT at the TSs involving carbonyl or imine derivatives. Note that the CT obtained at the reaction of unsubstituted benzaldehyde (**2c**) is similar to that found in the [3 + 2] cycloaddition reaction of **CYa** with *N*-methylisatin.[7] (ii) While at the reaction involving the imine **25a** the CT increases along the first stage of the reaction until **HPn1t**, the unexpected low CT observed in the reaction of benzaldehyde (**2c**) remains along the reaction.

Considering that the technical details and nomenclature of the ELF topological analysis are widely available,[27,28] we will concentrate our attention directly on its application[29,30] to the characterization of electron delocalization and the bonding pattern associated with **TSo1t** and **TSn1t** structures. Our aim is to further elucidate the electronic nature of charge rearrangement of these TSs associated with polar cycloaddition processes. The topological analysis of ELF for both TSs reveals the same structure of attractors (Figure 3). Focusing on the valence region, disynaptic basins associated with the bonding regions C4−X5, C1−O2, and O2−C3 appear. In addition, monosynaptic basins associated with the X5 and O2 atom in each TS emerge. A monosynaptic basin V(C3) associated with the atom C3 of **CYa** is also found in the reaction center of both TSs. This polarized monosynaptic basin V(C3) can be associated with the carbanionic center of the zwitterionic carbonyl ylide **CYa**. The basin populations associated with the V(C1,O2), V(C3,O2), and V(C4,X5) regions are 1.84, 1.40, and 1.98e for **TSo1t** and 1.81, 1.46, and 2.80e for **TSn1t**, respectively. The monosynaptic basins V(O2), V(X5), and V(C3) integrate 4.27, 5.44, and 1.05e in the case of **TSo1t** and 4.15, 2.70, and 0.94e in the case of **TSn1t**, respectively. These populations indicate a highly polarized electronic rearrangement. A complete analysis of the delocalization (not included here) reveals a greater fluctuation

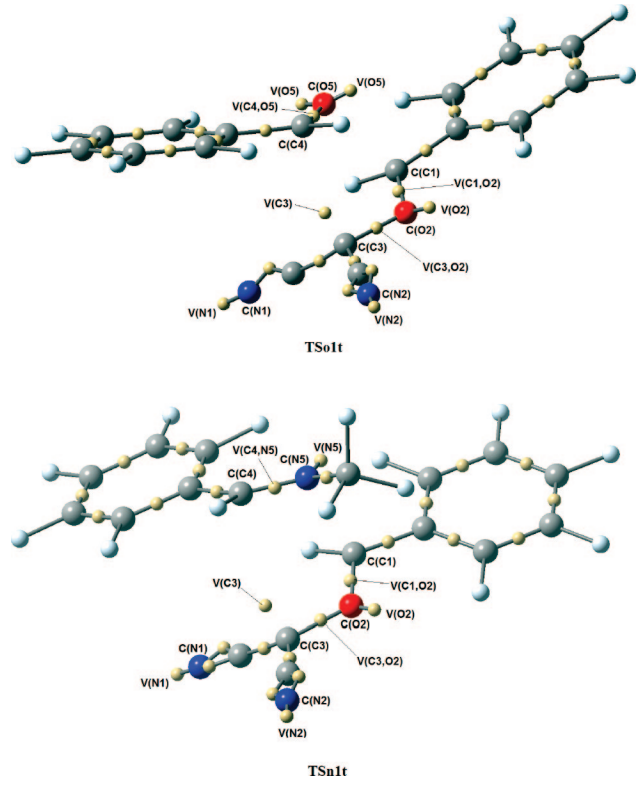

FIGURE 3. Spatial localization of the maxima (*e.g.*, attractors) of the electron localization function (ELF) for **TSo1t** and **TSn1t** (only attractors at the reaction center are labeled).

of electron populations between the valence basins in **TSo1t** than those observed in **TSn1t**. The electron density accumulated on the C3 center is, as noted above, higher at **TSo1t** than at **TSn1t**. This result can be rationalized by a large polarization of the former due to a back-donation process (see later). The ELF topological analysis of these two TSs does not reveal disynaptic basins that can be associated with the two new forming bonds (*e.g.*, C3−C4 and C1−X5). By considering a simple summation of electron and nuclei charges in the two separated reagent regions in both cases,[20] charge separations of 0.08 and 0.12e for **TSo1t** and **TSn1t** can be measured, respectively. The population analysis based on the topological regions shows that the ylide fragment is slightly positively charged in the case of **TSo1t** (+0.08e) and negatively charged in the case of **TSn1t** (−0.12e). These results are in complete agreement with those obtained through the NBO analysis made before. The polar nature and relative polarization of these TSs are also evident from the observed low bifurcation (η^*) values occurring between the two fragments in each case. As it has been previously emphasized,[20] the higher ELF bifurcation between two regions, the higher the electron delocalization between both regions is expected. In the present case, such bifurcations are associated with the C1−X5 and C3−C4 bonding domains, $\eta^*_{V(C3,C4)}$ and $\eta^*_{V(C1,X5)}$ (see Figure 4). For **TSo1t**, the bifurcation values are 0.375 and 0.358 for C1−X5 and C3−C4, respectively, while for **TSn1t**, the corresponding values are 0.460 and 0.100. Close bifurcation values for **TSo1t** can be traced out to a more synchronous electron charge rearrangement from O5 to C1 and from C3 to C4 (*e.g.*, back-donation as above-described). This effect is absent in the attack of N5 to C1 in **TSn1t**. As a result, a slightly higher accumulation of charge results in the monosynaptic region associated with the carbon

(27) (a) Savin, A.; Becke, A. D.; Flad, J.; Nesper, R.; Preuss, H.; Vonschnering, H. G. *Angew. Chem., Int. Ed. Engl.* **1991**, *30*, 409–412. (b) Savin, A.; Silvi, B.; Colonna, F. *Can. J. Chem.* **1996**, *74*, 1088–1096. (c) Savin, A.; Nesper, R.; Wengert, S.; Fassler, T. F. *Angew. Chem., Int. Ed. Engl.* **1997**, *36*, 1809–1832. (d) Silvi, B. *J. Mol. Struct.* **2002**, *614*, 3–10.

(28) (a) Bader, R. F. W.; Stephens, M. E. *J. Am. Chem. Soc.* **1975**, *97*, 7391–7399. (b) Fradera, X.; Austen, M. A.; Bader, R. F. W. *J. Phys. Chem. A* **1999**, *103*, 304–314. (c) Silvi, B. *Phys. Chem. Phys.* **2004**, *6*, 256–260.

(29) (a) Chamorro, E. *J. Chem. Phys.* **2003**, *118*, 8687–8698. (b) Chamorro, E.; Notario, R. *J. Phys. Chem. B* **2005**, *109*, 7594–7595. (c) Fuentealba, P.; Chamorro, E.; Santos, J. C. In *Theoretical Aspects of Chemical Reactivity*; Toro-Labbe, A., Ed.; Elsevier: Amsterdam, 2006; Vol. 19, p 57. (d) Chamorro, E.; Notario, R.; Santos, J. C.; Pérez, P. *Chem. Phys. Lett.* **2007**, *443*, 136–140.

(30) (a) Berski, S.; Andres, J.; Silvi, B.; Domingo, L. R. *J. Phys. Chem. A* **2003**, *107*, 6014–6024. (b) Polo, V.; Domingo, L. R.; Andres, J. *J. Phys. Chem. A* **2005**, *109*, 10438–10444. (c) Berski, S.; Andres, J.; Silvi, B.; Domingo, L. R. *J. Phys. Chem. A* **2006**, *110*, 13939–13947. (d) Polo, V.; Domingo, L. R.; Andres, J. *J. Org. Chem.* **2006**, *71*, 754–762. (e) Domingo, L. R.; Picher, M. T.; Arroyo, P.; Saez, J. A. *J. Org. Chem.* **2006**, *71*, 9319–9930.

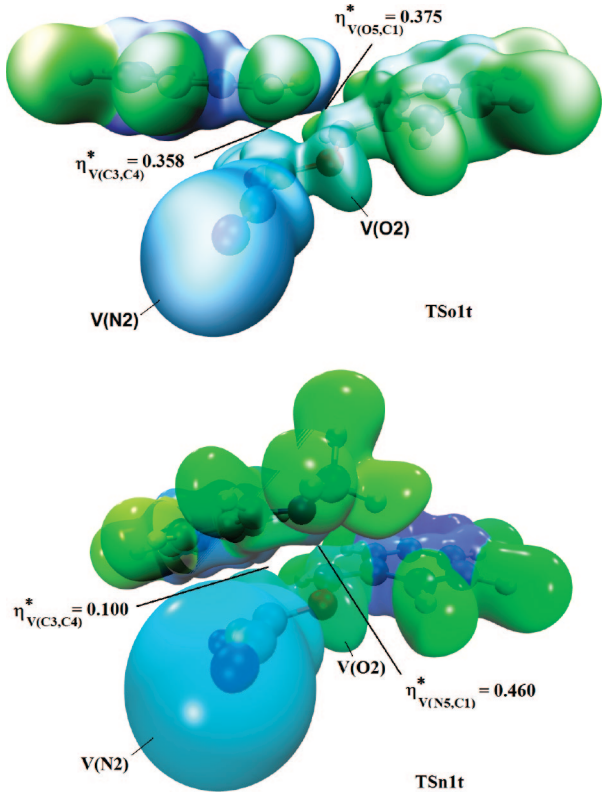

FIGURE 4. Electron localization function (ELF) isosurface pictures for **TSo1t** and **TSn1t**, indicating the bifurcation values at the region of bond formation. **TSo1t** exhibits a more synchronous pattern of delocalization at the region of new bond formation than **TSn1t** (see text for details).

atom C3 in **TSo1t**. **TSn1t** becomes more polar and more asynchronous with the formation of the two new bonds.

The ELF for **HPn1t** structure indicates that a disynaptic attractor can be associated with the formation of the C1−N5 bond, localizing 1.25e (see Figure 5). The monosynaptic valence attractor associated with the C3 atom remains monosynaptic in nature and it integrates to 0.99e in **HPn1t**. Therefore, it becomes clear that, on this pathway, the bond formation process is more asynchronous than that for the **TSo1t**. This picture supports the nonconcerted nature of the two-stage mechanism aforementioned: while a new disynaptic basin V(C1,N5) indicating the formation of the C1−N5 bond appears, the monosynaptic basin V(C3) remains at **TSn1t**.[30c] The basin populations associated with the V(C1,O2), V(C3,O2), and V(C4,N5) regions are 1.46, 1.36, and 2.48e, respectively. The monosynaptic attractors V(O2), V(N5), and V(C3) have populations of 4.61, 2.00, and 0.99e. As compared to **TSn1t**, the **HPn1t** structure is in fact more polarized. The population analysis based on the topological regions indicates that the negative charge at the ylide fragment increases to 0.27e. This result is in complete agreement with the NBO analysis made at **HPn1t** and discussed above. This fact further supports the idea that, along the reaction path associated with the **TSn1t**, the CT process is modulated by the initial attack of the N5 center to the C1 atom, opening the channel to the ring closure due to the attack of the C3 atom on the ylide to the C4 imine center.

The present theoretical study allows one to explain the mechanism of the [3 + 2] cycloaddition reactions of the carbonyl ylides as **CYa** as well as the unexpected reverse CT found at the reactions with aldehydes and ketones. The analysis

SCHEME 3. Flux of the CT at the TSs (the BO Values of the Forming Bonds are Given in Bold)

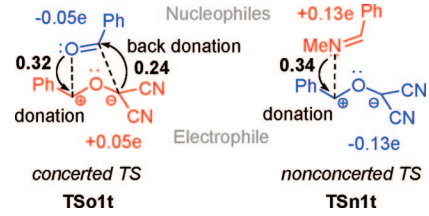

of the reactivity indexes indicates that both reagents involved in these [3 + 2] cycloadditions (carbonyl ylides and aldehydes or imines) have electrophilic/nucleophilic behaviors. However, the large electrophilic character of the carbonyl ylides makes us to think that these intermediates will act as electrophiles in polar processes. This analysis is in clear agreement with the NBO and ELF analysis of the electronic structure of **TSn1c**. At this nonconcerted TS, which is associated with the nucleophilic attack of the imine N5 nitrogen to the phenyl-substituted C1 carbon of the ylide, the CT fluxes clearly from the imine **25a** to **CYa** (see Scheme 3).

The NBO and ELF analysis of the CT at the concerted **TSo1c** appears to indicate that there is a change in the electrophilic/nucleophilic interaction. Now, the aldehyde **2c** appears to act as an electrophile, being negatively charged. However, the NBO and ELF analyses of the C1−O5 and C3−C4 forming bonds at **TSo1c** indicate that the C1−O5 bond formation is more advanced than the C3−C4 one. This behavior, which is in agreement with the analysis of the global and local reactivity indexes, points out that the nucleophilic attack of the O5 oxygen of the aldehyde **2c** to the electrophilically activated C1 center of **CYa** is more favored than the nucleophilic attack of the C3 carbon of **CYa** to the carbonyl C4 carbon of **2c**. That is, the reaction between **CYa** and the aldehyde **2c** implies a nucleophilic attack of aldehyde **2c** to **CYa**, but along this nucleophilic attack, the CT from the aldehyde **2c** to **CYa** increases the electrophilic character of the carbonyl C4 carbon, favoring a concerted back-donation from the nucleophilic C3 center of **CYa** (see ELF analysis) to the carbonyl C4 carbon. This phenomenon allows the nucleophilic attack of the aldehyde **2c** to **CYa** to progress and thus the whole cycloaddition process. This back-donation effect balances the net CT toward the aldehyde **2c** and allows further explanation of the unexpected reverse CT found in the [3 + 2] cycloaddition reactions involving these strong electrophilic ylides and carbonyl compounds as dienophiles. Note that, in spite of the low CT found at **TSo1t**, these cycloadditions have a large polar character.

In conclusion, we have shown that first 2,5-diaryl-1,3-dioxolane-4,4-dicarbonitriles and then 2,4-diphenyloxazolidine-5,5-dicarbonitriles can be prepared by regioselective cycloadditions between carbonyl ylides generated from epoxides. In contrast to the use of aldehydes, the reactions performed with imines proceed diastereoselectively.

The mechanism of the [3 + 2] cycloaddition reactions of the carbonyl ylides with aldehydes and imines has been theoretically studied using DFT methods. The analysis of the reactivity indexes indicates that both reagents involved in these [3 + 2] cycloadditions (carbonyl ylides and aldehydes or imines) have electrophilic/nucleophilic behaviors. However, the large electrophilic character of the carbonyl ylides makes them act as strong electrophiles in these polar processes. This behavior is supported by the NBO and ELF analyses of the electronic

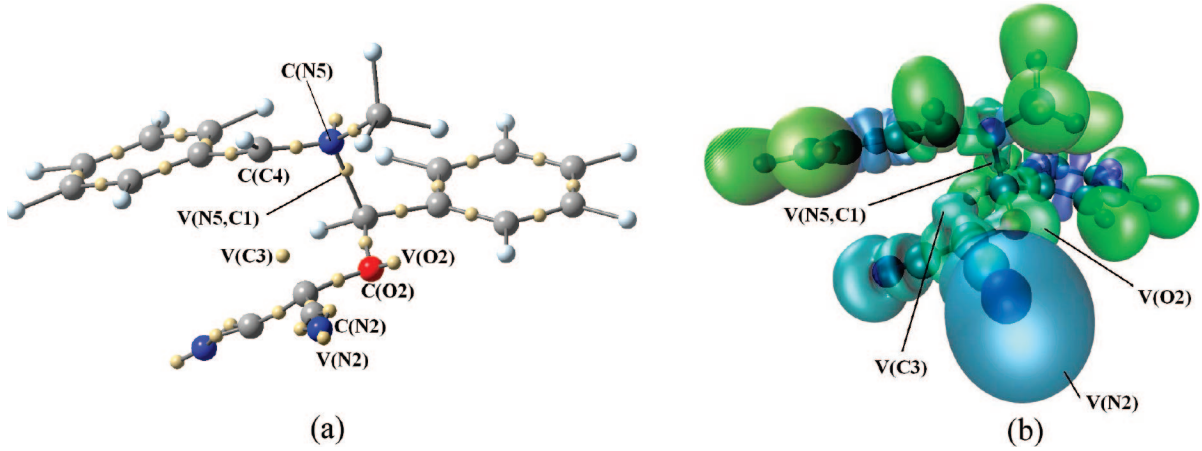

FIGURE 5. (a) Spatial localization of the maxima (*e.g.*, attractors) of the electron localization function (ELF) for **HPn1t** point along the reaction path associated with **TSn1t**. Only attractors at the reaction center are labeled. (b) ELF isosurface ($\eta = 0.728$) pictures for **HPn1t**.

structure of TSs involved in these reactions. The cycloaddition consists of the nucleophilic attack of the aldehyde oxygen or imine nitrogen atom to the carbonyl ylide. For the reaction with aldehydes, a back-donation effect that balances the net CT toward the carbonyl carbon atom allows one to explain the unexpected reverse CT found in the [3 + 2] cycloaddition reactions involving these strong electrophilic carbonyl ylides and carbonyl compounds acting as dienophiles.

Experimental Section

General Procedure 1 for the Reaction between Epoxides and Aldehydes Using Classical Heating. A mixture of epoxide (2.0 mmol) and aldehyde (2.0 mmol) in dry toluene (30 mL) was heated at reflux under N_2. The mixture was then evaporated to dryness and purified as specified in the product description.

General Procedure 2 for the Reaction between Epoxides and Aldehydes Using Microwave Irradiation. A mixture of epoxide (2.0 mmol) and aldehyde (2.0 mmol) was heated in the microwave oven (power, temperature, and time are given in the product description). The residue was purified as specified in the product description.

General Procedure 3 for the Reaction between Epoxides and Imines Using Classical Heating. A mixture of epoxide (2.0 mmol) and imine (2.0 mmol) in dry toluene (30 mL) was heated at reflux under N_2. The mixture was then evaporated to dryness. The residue was dissolved in a minimum of Et_2O. Upon addition of petrol, the precipitate formed was collected by filtration before recrystallization from Et_2O.

General Procedure 4 for the Reaction between Epoxides and Imines Using Microwave Irradiation. A mixture of epoxide (2.0 mmol) and imine (2.0 mmol) was heated in the microwave oven (power, temperature, and time are given in the product description). The residue was crystallized in Et_2O/petrol 20:80 and purified as specified in the product description.

Diastereoisomers of 5-(1-Naphthyl)-2-phenyl-1,3-dioxolane-4,4-dicarbonitrile (13a,b). The general procedure 1 (reflux of 80 h), using 3-phenyloxirane-2,2-dicarbonitrile (**1a**, 0.34 g) and 1-naphthaldehyde (**9**, 0.31 g), gave a 65/35 mixture from which the preponderant diastereoisomer **13a** was isolated by column chromatography over silica gel (eluent: petrol/AcOEt 90:10) in 27% yield as a white powder: mp 142 °C; ^{1}H NMR ($(CD_3)_2CO$) δ 6.70 (s, 1H), 7.07 (s, 1H), 7.7 (m, 8H), 8.2 (m, 3H), 8.40 (d, 1H, J = 8.4 Hz); ^{13}C NMR ($(CD_3)_2CO$) δ 70.4, 83.4, 108.1, 112.8, 114.0, 123.1, 126.3, 126.4, 127.5, 127.6, 128.3, 128.5 (2C), 129.8 (2C), 130.2, 131.2, 131.8, 132.0, 134.1, 134.8; HRMS *m/z* 326.1072 found (calcd for $C_{21}H_{14}N_2O_2$, $M^{+\bullet}$ requires 326.1055). The minor diastereoisomer **13b** was identified by the dioxolane ring ^{1}H NMR peaks: ^{1}H NMR ($(CD_3)_2CO$) δ 6.98 (s, 1H), 7.04 (s, 1H). The general procedure 2 (90 W, 12 min to reach 100 °C, 16 min to reach 120 °C, and 40 min at 120 °C), using 3-phenyloxirane-2,2-dicarbonitrile (**1a**, 0.34 g) and 1-naphthaldehyde (**9**, 0.31 g), gave a 62/38 mixture from which the preponderant diastereoisomer **13a** was isolated by column chromatography over silica gel (eluent: petrol/AcOEt 90:10) in 35% yield.

Diastereoisomers of 2-(4-Chlorophenyl)-5-(1-naphthyl)-1,3-dioxolane-4,4-dicarbonitrile (14a,b). The general procedure 1 (reflux of 72 h), using 3-(4-chlorophenyl)oxirane-2,2-dicarbonitrile (**1b**, 0.41 g) and 1-naphthaldehyde (**9**, 0.31 g), gave a 75/25 mixture from which the preponderant diastereoisomer **14a** was isolated by column chromatography over silica gel (eluent: petrol/AcOEt 90:10) in 32% yield as a beige powder: mp 178 °C; ^{1}H NMR ($(CD_3)_2CO$) δ 6.74 (s, 1H), 7.09 (s, 1H), 7.7 (m, 5H), 7.84 (d, 2H, J = 8.7 Hz), 8.10 (d, 2H, J = 7.5 Hz), 8.14 (d, 1H, J = 8.4 Hz), 8.37 (d, 1H, J = 8.4 Hz); ^{13}C NMR ($(CD_3)_2CO$) δ 70.4, 84.3, 107.2, 112.6, 113.9, 123.1, 126.3, 126.3, 126.4, 127.5, 128.3, 130.1 (2C), 130.3 (2C), 130.3, 131.1, 131.9, 133.0, 134.8, 137.5; HRMS *m/z* 360.0669 found (calcd for $C_{21}H_{13}N_2O_2{}^{35}Cl$, $M^{+\bullet}$ requires 360.0666). The minor diastereoisomer **14b** was identified by the dioxolane ring ^{1}H NMR peaks: ^{1}H NMR ($(CD_3)_2CO$) δ 7.01 (s, 1H), 7.07 (s, 1H). The general procedure 2 (90 W, 12 min to reach 100 °C, 16 min to reach 120 °C, and 40 min at 120 °C), using 3-(4-chlorophenyl)oxirane-2,2-dicarbonitrile (**1b**, 0.41 g) and 1-naphthaldehyde (**9**, 0.31 g), gave a 63/37 mixture from which the preponderant diastereoisomer **14a** was isolated by column chromatography over silica gel (eluent: petrol/AcOEt 90:10) in 42% yield.

Diastereoisomers of 2-(4-Methoxyphenyl)-5-(1-naphthyl)-1,3-dioxolane-4,4-dicarbonitrile (15a,b). The general procedure 1 (reflux of 57 h), using 3-(4-methoxyphenyl)oxirane-2,2-dicarbonitrile (**1c**, 0.40 g) and 1-naphthaldehyde (**9**, 0.31 g), gave a 76/24 mixture from which the preponderant diastereoisomer **15a** was isolated by column chromatography over silica gel (eluent: petrol/AcOEt 90:10) in 48% yield as a white powder: mp 155 °C; ^{1}H NMR ($(CD_3)_2CO$) δ 3.89 (s, 3H), 6.63 (s, 1H), 7.00 (s, 1H), 7.14 (d, 2H, J = 8.7 Hz), 7.7 (m, 5H), 8.1 (m, 3H), 8.38 (d, 1H, J = 8.4 Hz); ^{13}C NMR ($(CD_3)_2CO$) δ 55.8, 70.1, 84.1, 108.3, 112.9, 114.2, 115.2 (2C), 123.2, 125.9, 126.3, 126.4, 127.4, 127.8, 128.2, 130.2 (2C), 130.2, 131.2, 131.8, 134.8, 162.4; HRMS *m/z* 356.1189 found (calcd for $C_{22}H_{16}N_2O_3$, $M^{+\bullet}$ requires 356.1161). The minor diastereoisomer **15b** was identified by the dioxolane ring ^{1}H NMR peaks: ^{1}H NMR ($(CD_3)_2CO$) δ 6.96 (s, 1H), 6.98 (s, 1H). The general procedure 2 (90 W, 3 min to reach 60 °C, 6 min to reach 80 °C, and 30 min at 80 °C), using 3-(4-methoxyphenyl)oxirane-2,2-dicarbonitrile (**1c**, 0.40 g) and 1-naphthaldehyde (**9**, 0.31 g), gave a 71/29 mixture from which the preponderant diastereoisomer

15a was isolated by column chromatography over silica gel (eluent: petrol/AcOEt 90:10) in 55% yield.

Diastereoisomers of 5-(Indol-3-yl)-2-phenyl-1,3-dioxolane-4,4-dicarbonitrile (16a,b). The general procedure 1 (reflux of 84 h), using 3-phenyloxirane-2,2-dicarbonitrile (**1a**, 0.34 g) and indole-3-carboxaldehyde (**10**, 0.29 g), gave a 50/50 mixture from which the diastereoisomer **16a** was isolated by column chromatography over silica gel (eluent: petrol/AcOEt 75:25) in 40% yield as a red powder: mp 155 °C; ^{1}H NMR ($(CD_3)_2CO$) δ 6.43 (s, 1H), 6.61 (s, 1H), 7.2 (m, 2H), 7.6 (m, 4H), 7.8 (m, 4H), 10.88 (br s, 1H); ^{13}C NMR ($(CD_3)_2CO$) δ 70.7, 85.0, 105.3, 108.3, 113.0, 113.7, 114.0, 119.9, 121.1, 123.4, 126.4, 126.4, 128.4 (2C), 129.8 (2C), 131.8, 134.7, 137.7; HRMS *m/z* 315.1035 found (calcd for $C_{19}H_{13}N_3O_2$, $M^{+\bullet}$ requires 315.1008). The minor diastereoisomer **16b** was identified by its NMR and mass spectra: ^{1}H NMR ($(CD_3)_2CO$) δ 6.43 (s, 1H), 6.92 (s, 1H), 7.22 (t, 1H, J = 7.5 Hz), 7.29 (t, 1H, J = 7.5 Hz), 7.6 (m, 4H), 7.8 (m, 4H), 10.9 (br s, 1H); ^{13}C NMR ($(CD_3)_2CO$) δ 71.1, 82.6, 106.1, 107.9, 112.9, 114.0, 114.0, 120.0, 121.0, 123.4, 126.6, 127.4, 127.5 (2C), 129.7 (2C), 131.1, 136.3, 137.7; HRMS *m/z* 315.1035 found (calcd for $C_{19}H_{13}N_3O_2$, $M^{+\bullet}$ requires 315.1008). The general procedure 2 (90 W, 12 min to reach 100 °C, 16 min to reach 120 °C, and 45 min at 120 °C), using 3-phenyloxirane-2,2-dicarbonitrile (**1a**, 0.34 g) and indole-3-carboxaldehyde (**10**, 0.29 g), gave a 60/40 mixture from which the preponderant diastereoisomer **16a** was isolated by column chromatography over silica gel (eluent: petrol/AcOEt 75:25) in 42% yield.

Diastereoisomers of 2-(4-Chlorophenyl)-5-(indol-3-yl)-1,3-dioxolane-4,4-dicarbonitrile (17a,b). The general procedure 1 (reflux of 80 h), using 3-(4-chlorophenyl)oxirane-2,2-dicarbonitrile (**1b**, 0.41 g) and indole-3-carboxaldehyde (**10**, 0.29 g), gave a 43/57 mixture from which the diastereoisomer **17a** was isolated by column chromatography over silica gel (eluent: petrol/AcOEt 75:25) in 37% yield as an orange powder: mp 200 °C; ^{1}H NMR ($(CD_3)_2CO$) δ 6.45 (s, 1H), 6.63 (s, 1H), 7.21 (t, 1H, J = 7.2 Hz), 7.29 (t, 1H, J = 7.2 Hz), 7.60 (d, 1H, J = 8.1 Hz), 7.66 (d, 2H, J = 8.5 Hz), 7.82 (d, 2H, J = 8.4 Hz), 7.9 (m, 2H), 10.89 (br s, 1H); ^{13}C NMR ($(CD_3)_2CO$) δ 70.7, 85.0, 105.1, 107.3, 113.0, 113.6, 113.8, 119.9, 121.1, 123.4, 126.3, 126.4, 130.0 (2C), 130.1 (2C), 133.6, 137.3, 137.7; HRMS *m/z* 349.0637 found (calcd for $C_{19}H_{12}N_3O_2{}^{35}Cl$, $M^{+\bullet}$ requires 349.0618). The diastereoisomer **17b** was identified by NMR: ^{1}H NMR ($(CD_3)_2CO$) δ 6.44 (s, 1H), 6.93 (s, 1H), 7.19 (t, 1H, J = 7.3 Hz), 7.27 (t, 1H, J = 7.4 Hz), 7.7 (m, 7H), 10.9 (br s, 1H); ^{13}C NMR ($(CD_3)_2CO$) δ 71.1, 82.6, 106.0, 107.0, 112.8, 112.9, 113.9, 120.0, 121.0, 123.4, 126.5, 126.6, 129.3 (2C), 129.8 (2C), 135.3, 136.6, 137.6. The general procedure 2 (90 W, 12 min to reach 100 °C, 16 min to reach 120 °C, and 45 min at 120 °C), using 3-(4-chlorophenyl)oxirane-2,2-dicarbonitrile (**1b**, 0.41 g) and indole-3-carboxaldehyde (**10**, 0.29 g), gave a 76/24 mixture from which the preponderant diastereoisomer **17a** was isolated by column chromatography over silica gel (eluent: petrol/AcOEt 75:25) in 39% yield.

Diastereoisomers of 5-(Indol-3-yl)-2-(4-methoxyphenyl)-1,3-dioxolane-4,4-dicarbonitrile (18a,b). The general procedure 1 (reflux of 54 h), using 3-(4-methoxyphenyl)oxirane-2,2-dicarbonitrile (**1c**, 0.40 g) and indole-3-carboxaldehyde (**10**, 0.29 g), gave a 84/16 mixture from which the preponderant diastereoisomer **18a** was isolated by column chromatography over silica gel (eluent: petrol/AcOEt 75:25) in 46% yield as a greenish powder: mp 184 °C; ^{1}H NMR ($(CD_3)_2CO$) δ 3.91 (s, 3H), 6.37 (s, 1H), 6.54 (s, 1H), 7.14 (d, 2H, J = 8.7 Hz), 7.3 (m, 2H), 7.58 (d, 1H, J = 7.6 Hz), 7.72 (d, 2H, J = 8.7 Hz), 7.9 (m, 2H), 10.86 (br s, 1H); ^{13}C NMR ($(CD_3)_2CO$) δ 55.8, 70.6, 84.8, 105.4, 108.4, 113.0, 113.9, 114.1, 115.1 (2C), 120.0, 121.0, 123.4, 126.3, 126.3, 126.5, 130.0 (2C), 137.7, 162.7; HRMS *m/z* 288.1133 found (calcd for $C_{18}H_{14}N_3O$, $[M - H]^{+\bullet}$ requires 288.1133). The minor diastereoisomer **18b** was identified by its ^{1}H NMR spectra selected data: ^{1}H NMR ($(CD_3)_2CO$) δ 3.88 (s, 3H), 6.44 (s, 1H), 6.83 (s, 1H), 10.8 (br s, 1H). The general procedure 2 (120 W, 40 min at 80 °C), using 3-(4-methoxyphenyl)oxirane-2,2-dicarbonitrile (**1c**, 0.40 g) and indole-3-carboxaldehyde (**10**, 0.29 g), gave a 66/34 mixture from which the preponderant diastereoisomer **18a** was isolated by column chromatography over silica gel (eluent: petrol/AcOEt 75:25) in 30% yield.

Diastereoisomers of 5-(2-Furyl)-2-phenyl-1,3-dioxolane-4,4-dicarbonitrile (19a,b). The general procedure 1 (reflux of 50 h), using 3-phenyloxirane-2,2-dicarbonitrile (**1a**, 0.34 g) and 2-furaldehyde (**11**, 0.39 g, 0.33 mL, 4.0 mmol instead of 2.0 mmol), gave a 66/34 mixture from which the preponderant diastereoisomer **19a** was isolated by column chromatography over silica gel (eluent: Et_2O/heptane 30:70) in 36% yield as a white powder: mp 72 °C; ^{1}H NMR ($(CD_3)_2CO$) δ 6.17 (s, 1H), 6.53 (s, 1H), 6.64 (dd, 1H, J = 3.4 and 1.8 Hz), 6.99 (d, 1H, J = 3.4 Hz), 7.6 (m, 3H), 7.7 (m, 2H), 7.84 (d, 1H, J = 1.7 Hz); ^{13}C NMR ($(CD_3)_2CO$) δ 68.7, 82.4, 108.7, 112.1, 112.8, 113.2, 113.4, 128.4 (2C), 129.8 (2C), 132.0, 134.0, 144.4, 146.5; HRMS *m/z* 266.0690 found (calcd for $C_{15}H_{10}N_2O_3$, $M^{+\bullet}$ requires 266.0691). The minor diastereoisomer **19b** was identified by NMR: ^{1}H NMR ($(CD_3)_2CO$) δ 6.47 (s, 1H), 6.62 (dd, 1H, J = 3.2 and 1.8 Hz), 6.81 (s, 1H), 6.98 (d, 1H, J = 3.1 Hz), 7.5 (m, 3H), 7.7 (m, 2H), 7.82 (s, 1H); ^{13}C NMR ($(CD_3)_2CO$) δ 69.1, 81.3, 109.6, 111.9, 112.0, 114.3, 114.4, 128.1 (2C), 129.7 (2C), 131.7, 135.1, 146.2, 147.1.

Diastereoisomers of 2-(4-Chlorophenyl)-5-(2-furyl)-1,3-dioxolane-4,4-dicarbonitrile (20a,b). The general procedure 1 (reflux of 40 h), using 3-(4-chlorophenyl)oxirane-2,2-dicarbonitrile (**1b**, 0.41 g) and 2-furaldehyde (**11**, 0.39 g, 0.33 mL, 4.0 mmol instead of 2.0 mmol), gave a 67/33 mixture from which the minor diastereoisomer **20b** was isolated by column chromatography over silica gel (eluent: Et_2O/heptane 30:70) in 21% yield as white needles: mp 100 °C; ^{1}H NMR ($(CD_3)_2CO$) δ 6.48 (s, 1H), 6.83 (s, 1H), 6.61 (dd, 1H, J = 3.4 and 1.9 Hz), 6.95 (d, 1H, J = 3.4 Hz), 7.57 (d, 2H, J = 8.4 Hz), 7.68 (d, 2H, J = 8.4 Hz), 7.80 (d, 1H, J = 1.8 Hz); ^{13}C NMR ($(CD_3)_2CO$) δ 68.9, 81.3, 108.7, 111.9, 111.9, 114.3, 114.4, 129.9 (2C), 129.9 (2C), 134.0, 137.2, 146.3, 146.9; HRMS *m/z* 300.0319 found (calcd for $C_{15}H_9N_2O_3{}^{35}Cl$, $M^{+\bullet}$ requires 300.0302). The preponderant diastereoisomer **20a** was identified by NMR: ^{1}H NMR ($(CD_3)_2CO$) δ 6.17 (s, 1H), 6.55 (s, 1H), 6.64 (dd, 1H, J = 3.4 and 1.9 Hz), 6.99 (d, 1H, J = 3.4 Hz), 7.59 (d, 2H, J = 8.5 Hz), 7.71 (d, 2H, J = 8.5 Hz), 7.83 (d, 1H, J = 1.8 Hz); ^{13}C NMR ($(CD_3)_2CO$) δ 68.5, 82.2, 107.5, 111.9, 112.5, 112.9, 113.4, 129.8 (2C), 129.9 (2C), 132.6, 137.4, 144.0, 146.3.

Diastereoisomers of 5-(Furyl)-2-(4-methoxyphenyl)-1,3-dioxolane-4,4-dicarbonitrile (21a,b). The general procedure 1 (reflux of 35 h), using 3-(4-methoxyphenyl)oxirane-2,2-dicarbonitrile (**1c**, 0.40 g) and 2-furaldehyde (**11**, 0.39 g, 0.33 mL, 4.0 mmol instead of 2.0 mmol), gave a 65/35 mixture from which the minor diastereoisomer **21b** was isolated by column chromatography over silica gel (eluent: Et_2O/heptane 30:70) in 15% yield as a beige glitter: mp 85 °C; ^{1}H NMR ($(CD_3)_2CO$) δ 3.85 (s, 3H), 6.44 (s, 1H), 6.60 (dd, 1H, J = 3.3 and 1.8 Hz), 6.74 (s, 1H), 6.92 (d, 1H, J = 3.3 Hz), 7.05 (d, 2H, J = 8.8 Hz), 7.58 (d, 2H, J = 8.8 Hz), 7.59 (d, 1H, J = 1.8 Hz); ^{13}C NMR ($(CD_3)_2CO$) δ 55.6, 68.9, 81.1, 109.8, 111.9, 112.1, 114.2, 114.7, 115.1 (2C), 126.8, 129.9 (2C), 146.2, 147.4, 162.7; HRMS *m/z* 296.0792 found (calcd for $C_{16}H_{12}N_2O_4$, $M^{+\bullet}$ requires 296.0797). The preponderant diastereoisomer **21a** was identified by NMR: ^{1}H NMR ($(CD_3)_2CO$) δ 3.85 (s, 3H), 6.11 (s, 1H), 6.47 (s, 1H), 6.64 (dd, 1H, J = 3.3 and 1.8 Hz), 6.97 (d, 1H, J = 3.3 Hz), 7.08 (d, 2H, J = 8.7 Hz), 7.61 (d, 2H, J = 8.7 Hz), 7.83 (d, 1H, J = 1.1 Hz); ^{13}C NMR ($(CD_3)_2CO$) (selected data) δ 55.6, 68.4, 82.0, 108.6, 111.9, 114.8 (2C), 129.9 (2C), 144.3, 146.3, 162.7.

Diastereoisomers of 2-Phenyl-5-(2-thienyl)-1,3-dioxolane-4,4-dicarbonitrile (22a,b). The general procedure 1 (reflux of 48 h), using 3-phenyloxirane-2,2-dicarbonitrile (**1a**, 0.34 g) and thiophene-2-carboxaldehyde (**12**, 0.45 g, 0.37 mL, 4.0 mmol instead of 2.0 mmol), gave a 73/27 mixture from which the preponderant diastereoisomer **22a** was isolated by column chromatography over

silica gel (eluent: Et_2O/heptane 30:70) followed by recrystallization from petrol/Et_2O 50:50 in 40% yield as a white powder: mp 86 °C; ^1H NMR ($(CD_3)_2CO$) δ 6.40 (s, 1H), 6.56 (s, 1H), 7.25 (t, 1H, J = 4.0 Hz), 7.58 (s, 4H), 7.7 (m, 3H); ^{13}C NMR ($(CD_3)_2CO$) δ 70.9, 85.0, 108.7, 112.9, 113.2, 128.4 (2C), 128.6, 129.2, 129.4, 129.8 (2C), 132.1, 132.8, 134.1; HRMS m/z 282.0474 found (calcd for $C_{15}H_{10}N_2O_2S$, $M^{+\bullet}$ requires 282.0463). The minor diastereoisomer **22b** was isolated similarly in 20% yield as a greenish oil; ^1H NMR ($(CD_3)_2CO$) δ 6.47 (s, 1H), 6.87 (s, 1H), 7.22 (dd, 1H, J = 5.0 and 3.7 Hz), 7.5 (m, 4H), 7.6 (m, 2H), 7.73 (dd, 1H, J = 5.1 and 0.87 Hz); ^{13}C NMR ($(CD_3)_2CO$) δ 71.3, 83.2, 108.4, 112.0, 113.2, 127.5 (2C), 128.4, 129.4, 129.8, 129.7 (2C), 131.4, 133.7, 135.5.

Diastereoisomers of 2-(4-Chlorophenyl)-5-(2-thienyl)-1,3-dioxolane-4,4-dicarbonitrile (23a,b). The general procedure 1 (reflux of 41 h), using 3-(4-chlorophenyl)oxirane-2,2-dicarbonitrile (**1b**, 0.41 g) and thiophene-2-carboxaldehyde (**12**, 0.45 g, 0.37 mL, 4.0 mmol instead of 2.0 mmol), gave a 74/26 mixture from which the preponderant diastereoisomer **23a** was isolated by column chromatography over silica gel (eluent: Et_2O/heptane 30:70) followed by recrystallization from petrol/Et_2O 50:50 in 45% yield as a white powder: mp 150 °C; ^1H NMR ($(CD_3)_2CO$) δ 6.42 (s, 1H), 6.59 (s, 1H), 7.25 (dd, 1H, J = 5.0 and 3.7 Hz), 7.6 (m, 3H), 7.7 (m, 3H); ^{13}C NMR ($(CD_3)_2CO$) δ 70.7, 85.0, 107.7, 112.8, 113.0, 128.7, 129.3, 129.5, 130.1 (2C), 130.2 (2C), 132.7, 133.0, 137.6; HRMS m/z 316.0068 found (calcd for $C_{15}H_9N_2O_2{}^{35}ClS$, $M^{+\bullet}$ requires 316.0073). The minor diastereoisomer **23b** was isolated similarly in 25% yield as a colorless oil; ^1H NMR ($(CD_3)_2CO$) δ 6.49 (s, 1H), 6.90 (s, 1H), 7.23 (dd, 1H, J = 4.9 and 3.7 Hz), 7.6 (m, 3H), 7.68 (d, 2H, J = 8.5 Hz), 7.75 (dd, 1H, J = 5.1 and 0.96 Hz); ^{13}C NMR ($(CD_3)_2CO$) δ 71.3, 83.3, 107.7, 111.9, 113.2, 128.5, 129.5, 130.0, 129.4 (2C), 129.9 (2C), 133.6, 134.6, 136.9.

Diastereoisomers of 2-(4-Methoxyphenyl)-5-(2-thienyl)-1,3-dioxolane-4,4-dicarbonitrile (24a,b). The general procedure 1 (reflux of 36 h), using 3-(4-methoxyphenyl)oxirane-2,2-dicarbonitrile (**1c**, 0.40 g) and thiophene-2-carboxaldehyde (**12**, 0.45 g, 0.37 mL, 4.0 mmol instead of 2.0 mmol), gave a 62/38 mixture from which the preponderant diastereoisomer **24a** was isolated by column chromatography over silica gel (eluent: Et_2O/heptane 30:70) followed by recrystallization from petrol/Et_2O 50:50 in 50% yield as a pistachio powder: mp 88 °C; ^1H NMR ($(CD_3)_2CO$) δ 3.85 (s, 3H), 6.32 (s, 1H), 6.49 (s, 1H), 7.09 (d, 2H, J = 8.7 Hz), 7.24 (dd, 1H, J = 4.9 and 3.8 Hz), 7.56 (d, 1H, J = 3.4 Hz), 7.62 (d, 2H, J = 8.7 Hz), 7.73 (dd, 1H, J = 4.9 and 0.86 Hz); ^{13}C NMR ($(CD_3)_2CO$) δ 55.7, 70.7, 84.7, 108.7, 112.9, 113.2, 115.0 (2C), 125.7, 128.5, 128.9, 129.2, 130.0 (2C), 132.9, 162.8; HRMS m/z 312.0578 found (calcd for $C_{16}H_{12}N_2O_3S$, $M^{+\bullet}$ requires 312.0569). The minor diastereoisomer **24b** was isolated similarly in 20% yield as colorless crystals: mp 82 °C; ^1H NMR ($(CD_3)_2CO$) δ 3.86 (s, 3H), 6.48 (s, 1H), 6.81 (s, 1H), 7.06 (d, 2H, J = 8.8 Hz), 7.22 (dd, 1H, J = 5.1 and 3.7 Hz), 7.55 (d, 1H, J = 3.6 Hz), 7.59 (d, 2H, J = 8.8 Hz), 7.74 (dd, 1H, J = 5.1 and 1.1 Hz); ^{13}C NMR ($(CD_3)_2CO$) δ 55.8, 71.3, 83.2, 108.8, 112.1, 113.5, 115.1 (2C), 127.4, 128.5, 129.4, 129.9, 129.4 (2C), 134.1, 162.6; HRMS m/z 312.0575 found (calcd for $C_{16}H_{12}N_2O_3S$, $M^{+\bullet}$ requires 312.0569).

Crystallography: The crystals were obtained by slowly evaporating acetone solutions.

Crystal data for **5a** (colorless prisms): $C_{21}H_{20}N_2O_6$, M_r = 396.39, monoclinic, space group $P2_1$, a = 7.8658(7), b = 8.6374(8), c = 15.3824(16) Å, β = 99.533(5)°, V = 1030.65(17) Å^3, Z = 2, ρ_{calcd} = 1.277 g·cm^{-3}, μ = 0.095 mm^{-1}. A final refinement on F^2 with 2497 unique intensities and 262 parameters converged at $\omega R(F^2)$ = 0.0812 ($R(F)$ = 0.0359) for 2359 observed reflections with $I > 2\sigma(I)$. Crystallographic data were deposited in CSD under CCDC registration number 688228.

Crystal data for **6a** (colorless prisms): $C_{18}H_{12}N_2O_4$, M_r = 320.30, monoclinic, space group $P2_1/a$, a = 13.4303(7), b = 7.8903(4), c = 13.9246(6) Å, β = 91.425(3)°, V = 1475.12(12) Å^3, Z = 4, ρ_{calcd} = 1.442 g·cm^{-3}, μ = 0.104 mm^{-1}. A final refinement on F^2 with 3377 unique intensities and 217 parameters converged at $\omega R(F^2)$ = 0.0885 ($R(F)$ = 0.0391) for 2781 observed reflections with $I > 2\sigma(I)$. Crystallographic data were deposited in CSD under CCDC registration number 688219.

Crystal data for **6b** (colorless prisms): $C_{18}H_{12}N_2O_4$, M_r = 320.30, orthorhombic, space group $Pbca$, a = 8.2939(5), b = 12.8750(6), c = 27.3006(14) Å, V = 2915.3(3) Å^3, Z = 8, ρ_{calcd} = 1.46 g·cm^{-3}, μ = 0.105 mm^{-1}. A final refinement on F^2 with 3346 unique intensities and 217 parameters converged at $\omega R(F^2)$ = 0.1126 ($R(F)$ = 0.0471) for 3129 observed reflections with $I > 2\sigma(I)$. Crystallographic data were deposited in CSD under CCDC registration number 688216.

Crystal data for **7a** (colorless prisms): $C_{18}H_{11}ClN_2O_4$, M_r = 354.74, monoclinic, space group $P2_1/a$, a = 13.7192(7), b = 7.4109(4), c = 15.3928(7) Å, β = 93.948(2)°, V = 1561.30(14) Å^3, Z = 4, ρ_{calcd} = 1.509 g·cm^{-3}, μ = 0.272 mm^{-1}. A final refinement on F^2 with 3547 unique intensities and 226 parameters converged at $\omega R(F^2)$ = 0.0894 ($R(F)$ = 0.0353) for 2987 observed reflections with $I > 2\sigma(I)$. Crystallographic data were deposited in CSD under CCDC registration number 688218.

Crystal data for **8a** (colorless prisms): $C_{19}H_{14}N_2O_5$, M_r = 350.32, monoclinic, space group $P2_1/a$, a = 13.9650(6), b = 7.3292(3), c = 15.6911(6) Å, β = 95.712(2)°, V = 1598.05(11) Å^3, Z = 4, ρ_{calcd} = 1.456 g·cm^{-3}, μ = 0.107 mm^{-1}. A final refinement on F^2 with 3654 unique intensities and 236 parameters converged at $\omega R(F^2)$ = 0.0912 ($R(F)$ = 0.0358) for 3085 observed reflections with $I > 2\sigma(I)$. Crystallographic data were deposited in CSD under CCDC registration number 688223.

Crystal data for **17a** (colorless prisms): $C_{19}H_{12}ClN_3O_2$, M_r = 349.77, monoclinic, space group $C2/c$, a = 8.7943(18), b = 18.422(4), c = 19.814(4) Å, β = 92.353(9)°, V = 3207.3(12) Å^3, Z = 8, ρ_{calcd} = 1.449 g·cm^{-3}, μ = 0.256 mm^{-1}. A final refinement on F^2 with 3662 unique intensities and 229 parameters converged at $\omega R(F^2)$ = 0.1389 ($R(F)$ = 0.0525) for 3113 observed reflections with $I > 2\sigma(I)$. Crystallographic data were deposited in CSD under CCDC registration number 688214.

Crystal data for **20b** (colorless prisms): $C_{15}H_9ClN_2O_3$, M_r = 300.69, monoclinic, space group $P2_1/a$, a = 5.8491(3), b = 27.7737(12), c = 8.3610(4) Å, β = 95.084(2)°, V = 1352.91(11) Å^3, Z = 4, ρ_{calcd} = 1.476 g·cm^{-3}, μ = 0.294 mm^{-1}. A final refinement on F^2 with 3097 unique intensities and 190 parameters converged at $\omega R(F^2)$ = 0.0955 ($R(F)$ = 0.0375) for 2776 observed reflections with $I > 2\sigma(I)$. Crystallographic data were deposited in CSD under CCDC registration number 688222.

Crystal data for **24a** (colorless prisms): $C_{16}H_{12}N_2O_3S$, M_r = 312.34, triclinic, space group $P1,^-$ a = 8.7692(5), b = 10.0582(6), c = 10.4679(6) Å, α = 115.933(2), β = 92.721(3), γ = 112.118(2)°, V = 743.87(7) Å^3, Z = 2, ρ_{calcd} = 1.394 g·cm^{-3}, μ = 0.231 mm^{-1}. A final refinement on F^2 with 3371 unique intensities and 200 parameters converged at $\omega R(F^2)$ = 0.081 ($R(F)$ = 0.0315) for 3117 observed reflections with $I > 2\sigma(I)$. Crystallographic data were deposited in CSD under CCDC registration number 688221.

Crystal data for **29a** (colorless prisms): $C_{18}H_{14}N_4O_3$, M_r = 334.33, monoclinic, space group $P2_1/n$, a = 7.2945(6), b = 12.4389(12), c = 18.2616(18) Å, β = 96.102(5)°, V = 1647.6(3) Å^3, Z = 4, ρ_{calcd} = 1.348 g·cm^{-3}, μ = 0.095 mm^{-1}. A final refinement on F^2 with 3766 unique intensities and 226 parameters converged at $\omega R(F^2)$ = 0.1076 ($R(F)$ = 0.0431) for 3118 observed reflections with $I > 2\sigma(I)$. Crystallographic data were deposited in CSD under CCDC registration number 688229.

Crystal data for **31a** (colorless plates): $C_{21}H_{18}ClN_3O_3$, M_r = 395.83, monoclinic, space group $P2_1$, a = 7.1324(9), b = 7.4170(9), c = 18.265(2) Å, β = 101.203(6)°, V = 947.8(2) Å^3, Z = 2, ρ_{calcd} = 1.387 g·cm^{-3}, μ = 0.229 mm^{-1}. A final refinement on F^2 with 3807 unique intensities and 255 parameters converged at $\omega R(F^2)$ = 0.1125 ($R(F)$ = 0.049) for 3239 observed reflections with $I > 2\sigma(I)$. Crystallographic data were deposited in CSD under CCDC registration number 688215.

Crystal data for **32a** (yellow prisms): $C_{22}H_{21}N_3O_4$, $M_r = 391.42$, orthorhombic, space group *Pbca*, $a = 11.4248(8)$, $b = 15.8816(11)$, $c = 21.3075(16)$ Å, $V = 3866.1(5)$ Å^3, $Z = 8$, $\rho_{calcd} = 1.345$ g·cm^{-3}, $\mu = 0.094$ mm^{-1}. A final refinement on F^2 with 4413 unique intensities and 262 parameters converged at $\omega R(F^2) = 0.1319$ ($R(F) = 0.0649$) for 3127 observed reflections with $I > 2\sigma(I)$. Crystallographic data were deposited in CSD under CCDC registration number 688227.

Crystal data for **33a** (colorless prisms): $C_{21}H_{18}N_4O_5$, $M_r = 406.39$, orthorhombic, space group *Pbca*, $a = 7.0163(10)$, $b = 13.875(2)$, $c = 39.050(5)$ Å, $V = 3801.6(9)$ Å^3, $Z = 8$, $\rho_{calcd} = 1.42$ g·cm^{-3}, $\mu = 0.104$ mm^{-1}. A final refinement on F^2 with 4341 unique intensities and 271 parameters converged at $\omega R(F^2) = 0.1123$ ($R(F) = 0.0455$) for 3640 observed reflections with $I > 2\sigma(I)$. Crystallographic data were deposited in CSD under CCDC registration number 688230.

Crystal data for **39a** (colorless prisms): $C_{25}H_{18}ClN_3O_3$, $M_r = 443.87$, monoclinic, space group $P2_1/a$, $a = 13.6352(16)$, $b = 7.6099(8)$, $c = 21.144(2)$ Å, $\beta = 105.610(6)°$, $V = 2113.0(4)$ Å^3, $Z = 4$, $\rho_{calcd} = 1.395$ g·cm^{-3}, $\mu = 0.214$ mm^{-1}. A final refinement on F^2 with 4809 unique intensities and 289 parameters converged at $\omega R(F^2) = 0.1578$ ($R(F) = 0.0777$) for 4030 observed reflections with $I > 2\sigma(I)$. Crystallographic data were deposited in CSD under CCDC registration number 688226.

Computational Methods: All calculations were carried out with the Gaussian 03 suite of programs.[31] DFT calculations were carried out using the B3LYP[32] exchange-correlation functionals, together with the standard 6-31G* basis set.[33] This level of theory has shown to be suitable to provide good enough performance in the analysis of both geometric and electronic properties in cycloaddition reactions. The stationary points were characterized by frequency calculations in order to verify that TSs had one and only one imaginary frequency. The intrinsic reaction coordinate (IRC)[34] path was traced in order to check the energy profiles connecting each TS to the two associated minima of the proposed mechanism using the second order González−Schlegel integration method.[35] The electronic structures of stationary points were analyzed by the NBO method[36] and the topological analysis of the ELF, $\eta(\mathbf{r})$.[27] The ELF study was performed with the TopMod program[37] using the corresponding monodeterminantal wave functions of transition state structures.

Solvent effects have been considered by B3LYP/6-31G* single-point calculations on the gas-phase structures using a self-consistent reaction field (SCRF)[38] based on the polarizable continuum model (PCM) of Tomasi's group.[39] Since these reactions are carried out in toluene, we have selected its dielectric constant at 298.0 K, $\varepsilon = 2.38$.

The global electrophilicity index,[19] ω, which measures the energy stabilization when the system acquires an additional electronic charge ΔN from the environment, is given by the following simple expression, $\omega = (\mu^2/2\eta)$, in terms of the electronic chemical potential μ and the chemical hardness η. These quantities may be approached in terms of the energies of the frontier molecular orbital HOMO and LUMO, ε_H and ε_L, as $\mu \approx (\varepsilon_H + \varepsilon_L)/2$ and $\eta \approx (\varepsilon_L - \varepsilon_H)$, respectively.[40] Recently, we have introduced an empirical (relative) nucleophilicity index, N, based on the HOMO energies obtained within the Kohn−Sham scheme, and defined as $N = \varepsilon_{HOMO(Nu)} - \varepsilon_{HOMO(TCE)}$, where tetracyanoethylene (TCE) is chosen as reference.[20]Local electrophilicity[22] and nucleophilicity[24] indexes, ω_k and N_k, were evaluated using the following expressions: $\omega_k = \omega f_k^+$ and $N_k = N f_k^-$, where f_k^+ and f_k^- are the Fukui functions for a nucleophilic and electrophilic attacks, respectively.[23]

Acknowledgment. We are grateful to the Spanish Government (project CTQ2006-14297/BQU), the Algerian MESRS for PROFAS financial support to G.B.-A., and the Fondecyt Projects Nos. 1060961 (P.P.) and 1070378 (E.C.). E.C. and P.P. also thank the Universidad Andrés Bello (UNAB) for support through project DI 21-06/R and 45-08/R, respectively. L.R.D. also thanks the Fondecyt Grant No. 7080026 (Cooperación Internacional) for financial support, and the Universidad Andrés Bello for its hospitality. We thank Jean Pierre Bazureau for generous microwave access. We thank Sourisak Sinbandhit for his contribution to this study.

Supporting Information Available: General methods, starting materials, compound characterizations, crystallography, ORTEP diagrams, copies of the ^{1}H and ^{13}C NMR spectra for compounds **13a**−**24a**, geometries of the TSs with the (*Z*)-imine **25a**, B3LYP/6-31G* computed total energies, unique imaginary frequencies, Cartesian coordinates of the TSs and cycloadducts, and CIF files of **5a**, **6a**, **6b**, **7a**, **8a**, **17a**, **20b**, **24a**, **29a**, **31a**, **32a**, **33a**, and **39a**. This material is available free of charge via the Internet at http://pubs.acs.org.

JO8027104

(31) Frisch, M. J.; Trucks, G. W.; Schlegel, H. B.; Scuseria, G. E.; Robb, M. A.; Cheeseman, J. R.; Montgomery, J. A., Jr.; Vreven, T.; Kudin, K. N.; Burant, J. C.; Millam, J. M.; Iyengar, S. S.; Tomasi, J.; Barone, V.; Mennucci, B.; Cossi, M.; Scalmani, G.; Rega, N.; Petersson, G. A.; Nakatsuji, H.; Hada, M.; Ehara, M.; Toyota, K.; Fukuda, R.; Hasegawa, J.; Ishida, M.; Nakajima, T.; Honda, Y.; Kitao, O.; Nakai, H.; Klene, M.; Li, X.; Knox, J. E.; Hratchian, H. P.; Cross, J. B.; Adamo, C.; Jaramillo, J.; Gomperts, R.; Stratmann, R. E.; Yazyev, O.; Austin, A. J.; Cammi, R.; Pomelli, C.; Ochterski, J. W.; Ayala, P. Y.; Morokuma, K.; Voth, G. A.; Salvador, P.; Dannenberg, J. J.; Zakrzewski, V. G.; Dapprich, S.; Daniels, A. D.; Strain, M. C.; Farkas, O.; Malick, D. K.; Rabuck, A. D.; Raghavachari, K.; Foresman, J. B.; Ortiz, J. V.; Cui, Q.; Baboul, A. G.; Clifford, S.; Cioslowski, J.; Stefanov, B. B.; Liu, G.; Liashenko, A.; Piskorz, P.; Komaromi, I.; Martin, R. L.; Fox, D. J.; Keith, T.; Al-Laham, M. A.; Peng, C. Y.; Nanayakkara, A.; Challacombe, M.; Gill, P. M. W.; Johnson, B.; Chen, W.; Wong, M. W.; Gonzalez, C.; Pople, J. A. *Gaussian03*; Gaussian, Inc.: Wallingford CT, 2004.

(32) (a) Becke, A. D. *J. Chem. Phys.* **1993**, *98*, 5648–5652. (b) Lee, C.; Yang, W.; Parr, R. G. *Phys. Rev. B* **1988**, *37*, 785–789.

(33) Hehre, W. J.; Radom, L.; Schleyer, P. v. R.; Pople, J. A. *Ab initio Molecular Orbital Theory*; Wiley: New York, 1986.

(34) Fukui, K. *J. Phys. Chem.* **1970**, *74*, 4161–4163.

(35) (a) González, C.; Schlegel, H. B. *J. Phys. Chem.* **1990**, *94*, 5523–5527. (b) González, C.; Schlegel, H. B. *J. Chem. Phys.* **1991**, *95*, 5853–5860.

(36) (a) Reed, A. E.; Curtiss, L. A.; Weinhold, F. *Chem. Rev.* **1988**, *88*, 899–926. (b) Reed, A. E.; Weinstock, R. B.; Weinhold, F. *J. Chem. Phys.* **1985**, *83*, 735–746.

(37) Noury, S.; Krokidis, X.; Fuster, F.; Silvi, B. *Comput. Chem.* **1999**, *23*, 597–604.

(38) (a) Tomasi, J.; Persico, M. *Chem. Rev.* **1994**, *94*, 2027–2094. (b) Simkin, B. Y.; Sheikhet, I. *Quantum Chemical and Statistical Theory of Solutions-A Computational Approach*; Ellis Harwood: London, 1995.

(39) (a) Cances, E.; Mennucci, B.; Tomasi, J. *J. Chem. Phys.* **1997**, *107*, 3032–3041. (b) Cossi, M.; Barone, V.; Cammi, R.; Tomasi, J. *Chem. Phys. Lett.* **1996**, *255*, 327–335. (c) Barone, V.; Cossi, M.; Tomasi, J. *J. Comput. Chem.* **1998**, *19*, 404–417.

(40) (a) Parr, R. G.; Pearson, R. G. *J. Am. Chem. Soc.* **1983**, *105*, 7512–7516. (b) Parr, R. G.; Yang, W. *Density Functional Theory of Atoms and Molecules*; Oxford University Press: New York, 1989.